Film Implementation of a Neutron Detector (FIND): Critical Materials Properties

W. C. McGinnis
SSC San Diego

R. Clarke
C. Cionca
University of Michigan

SSC San Diego

TECHNICAL REPORT 1957
September 2007

Film Implementation of a Neutron Detector (FIND): Critical Materials Properties

W. C. McGinnis
SSC San Diego

R. Clarke
C. Cionca
University of Michigan

SPAWAR
Systems Center
San Diego

SSC San Diego
San Diego, CA 92152-5001

SSC SAN DIEGO
San Diego, California 92152-5001

F. D. Unetic, CAPT USN
Commanding Officer

C. A. Keeney
Technical Director

ADMINISTRATIVE INFORMATION

The work described in this report was performed for the Domestic Nuclear Detection Office, Department of Homeland Security by the Applied Research Branch, Code 2373, Space and Naval Warfare Systems Center San Diego (SSC San Diego).

Released under authority of
G. Anderson, Head
Applied Research Branch

Released under authority of
M. Machniak, Head
Advanced Systems & Applied
Sciences Division

The citation of trade names and names of manufacturers in this report is not to be construed as official government endorsement or approval of commercial products or services referenced in this report.

Amptek® is a registered trademark of Amptek, Inc.
Combat® is a registered trademark of Saint-Gobain Ceramics & Plastics, Inc.
Keithley® is a registered trademark of Keithley Instruments, Inc.

SB

ACKNOWLEDGMENTS

EXECUTIVE SUMMARY

OBJECTIVE

The Film Implementation of a Neutron Detector (FIND) project is a research and development investigation of a new type of solid-state thermal neutron detector, potentially providing improvements in sensitivity, size, weight, power consumption, operator safety, transportability, and cost compared to current neutron detector technology. The objective of this project phase is to develop a reproducible FIND device based on insulating boron nitride (BN) films or thin sheets, guided by the key materials properties needed for a workable device.

RESULTS

The techniques needed to measure the key BN electrical properties of carrier lifetime and mobility were developed and implemented. Acceptable values of these properties, as well as reasonably good electrical contact to BN and sufficiently high BN resistivity, are needed for a working FIND device. Initial measurements of these key properties were made using the following methods:

- Lifetime: time-resolved (pump-probe) reflectivity method with dual fiber laser system
- Mobility: free-surface charging with corona triode system .

This phase of the project focused on BN sample deposition/preparation and characterization. Only limited testing of detectors based on these BN samples has been carried out at this point. Two BN samples (one a freestanding pyrolytic BN sheet and the other a hexagonal BN film deposited on a silicon substrate) were configured and tested as FIND devices, but with a null result for thermal neutron detection. A measured carrier lifetime value of 40 ps for the pyrolytic sample explains this result. The hexagonal film has a much higher carrier lifetime (3 ns), but initial measurements indicate a very poor mobility value for that sample, and so free carriers generated by a neutron-boron reaction do not reach the detector electrodes. Based on previous measurements of semiconducting film samples, much higher mobilities are expected for cubic BN films. In addition, carrier lifetimes of several nanoseconds have been measured in cubic phase films.

Finally, an SSC San Diego invention disclosure has been submitted for a detector capable of determining the incident direction of thermal neutrons. The omnidirectional detector would be formed from three orthogonal pairs of planar BN detector elements (FIND devices).

RECOMMENDATIONS

Continuation of the work described above is needed to make a reproducible and reliable FIND device for detecting thermal neutrons. The newly applied sample characterization techniques, along with ongoing improvements in BN film growth, can be used to test and optimize a solid-state detection element based on high-quality cubic boron nitride films. Based on the data reported here, of the various available forms of BN, cubic phase films seem to hold the most promise. Once individual FIND devices have been optimized, multiple FIND elements can be combined into a thermal neutron detector with directional capability.

CONTENTS

Figures

INTRODUCTION

PROBLEM ADDRESSED AND INVESTIGATED SOLUTION

The research described in this report addresses the need for efficient and convenient inspection of buildings, vehicles, persons, and other places for concealed nuclear materials (such as uranium or plutonium) that are used or capable of being used in nuclear weapons. One way to determine the presence of nuclear materials is to detect the neutrons that are emitted from the atomic nucleus of these materials in the radioactive decay process. To overcome the problems encountered with conventional detectors, a solid-state analog of the gas proportional counter based on films or thin sheets of boron nitride (BN) was investigated. This new type of detector[1] is known as a Film Implementation of a Neutron Detector (FIND). The term "film" is meant to include thin sheets as well.

BACKGROUND

This research is a continuation of the 2002–2003 effort in which a prototype FIND device, based on a thin bulk BN detecting element, was demonstrated to be sensitive to irradiation by thermal neutrons.[2,*]

Neutrons can be detected by measurement of the secondary charged particles that result from nuclear reactions such as

$$n + {}^{10}B \rightarrow {}^{7}Li^* + \alpha \quad ; \quad {}^{7}Li^* \rightarrow {}^{7}Li + \gamma \ . \tag{1}$$

The 1.47-MeV alpha particles from this reaction create electron-hole pairs in the material. Detection of these charge carriers before they recombine indicates the presence of the incident neutrons. The isotope boron-10, with its relatively large cross section for thermal neutrons (3837 barns), is particularly well suited for neutron detection, and is commonly used in gas-type counter detectors in the form of boron trifluoride gas, BF_3. Because of its greater density, a boron-containing solid detector would have a greatly enhanced total cross section for neutrons, and thus far better detector sensitivity. For example, the total cross section increases by a factor of about 3000 in going from BF_3 gas (at room temperature and atmospheric pressure) to solid boron nitride. In addition, the wide band gap of BN (around 5 to 6 eV) means better room temperature operation than semiconductor solid-state nuclear particle detectors due to reduced thermally induced recombination of electrons and holes, as well as greatly reduced background noise from thermal excitation of electron-hole pairs. Finally, pure BN is a very stable, chemically inert compound that can withstand large variations in temperature and humidity without degradation, and thus is suitable for use in a portable detector unit that could be deployed in varied environments.

Compared to commonly used neutron detectors, such as gas proportional and scintillation counters, the FIND device is much more compact, and therefore portable. The detecting element consists of a substrate that supports a boron nitride film sandwiched by electrode layers. The total thickness of the detector element is typically less than 1 mm. The area of a single detector element is 1 cm^2 or smaller (depending on the BN thickness and resistivity). Large area detectors would consist of an array or mosaic of single detector elements. Because the voltage applied across the BN film is on the order of a few volts, compared to kilovolts for standard detectors, problems associated with high

---

*[*] The introductory and background material included here are also in the 2003 report.[2] See the latter for details on modeling of the FIND device.

voltage (arcing and the extra space or insulation needed to prevent arcing) are avoided. Operation at low voltage also means that the electronics used to apply the electrode voltage and measure the detector current can be simpler, more compact, safer to the user, and much less power consuming. BN also has an unusually large dielectric breakdown strength ($\sim$ 35 kV/mm), advantageous to detector operation in a thin film geometry. Electronic noise caused by environmental vibrations, a common problem with gas proportional counters, is non-existent in this solid-state device. Additionally, the FIND device does not use exotic high-purity gases (or the special means to contain the gases at high pressure) required by gas proportional counter detectors. Solid-state neutron detectors based on silicon (Si) or germanium photodiodes and phototransistors have been designed also, but they are much smaller in area than the FIND device, and therefore less sensitive. They also require a neutron converter foil such as gadolinium in front of the semiconductor device, which further limits detector efficiency and sensitivity.

PROJECT PERSONNEL

The boron nitride films studied in this research were grown and characterized in various ways by the University of Michigan (under SSC San Diego contract number N66001-03-D-0041, delivery order 6). The University of Michigan (UMich) personnel involved in this effort include Dr. Roy Clarke (professor in experimental materials and condensed matter physics), Dr. Codrin Cionca (research scientist), and Vladimir Stoica (graduate research assistant). Staff in the UMich electron microbeam analysis facility and in the Michigan Solid State Electronics Research Lab helped process and characterize samples for the project.

The remainder of the project tasks were performed at SSC San Diego. The primary SSC San Diego personnel working on this project are Dr. Wayne McGinnis, Mark Kottke (graduate student contractor; doctoral candidate in the Department of Chemistry and Biochemistry at University of California, San Diego; graduate student assistant in the Department of Chemistry and Biochemistry at San Diego State University), David Ponte (graduate student contractor; masters candidate in the Department of Chemistry and Biochemistry at San Diego State University), and Dr. Manjit Randhawa (visiting professor from Southern University, Baton Rouge). Marc Rasmussen (SSC San Diego Code 2741) acted as administrative liaison to the sponsor, the Department of Homeland Security. Ron Brockus (SSC San Diego Code 2741) assisted with handling of the americium-beryllium (Am-Be) neutron source used for detector testing.

FIND DEVICE DESCRIPTION

A schematic representation of the FIND detector circuit is shown in Figure 1. Current is measured with the ammeter, and the resistor value is chosen to control the voltage drop across the BN film. The over-simplified circuit shown would be useful only for neutron flux levels high enough to generate a steady current that flows in addition to the background or dark current. The total measured current is the sum of the dark current and this additional or excess current.
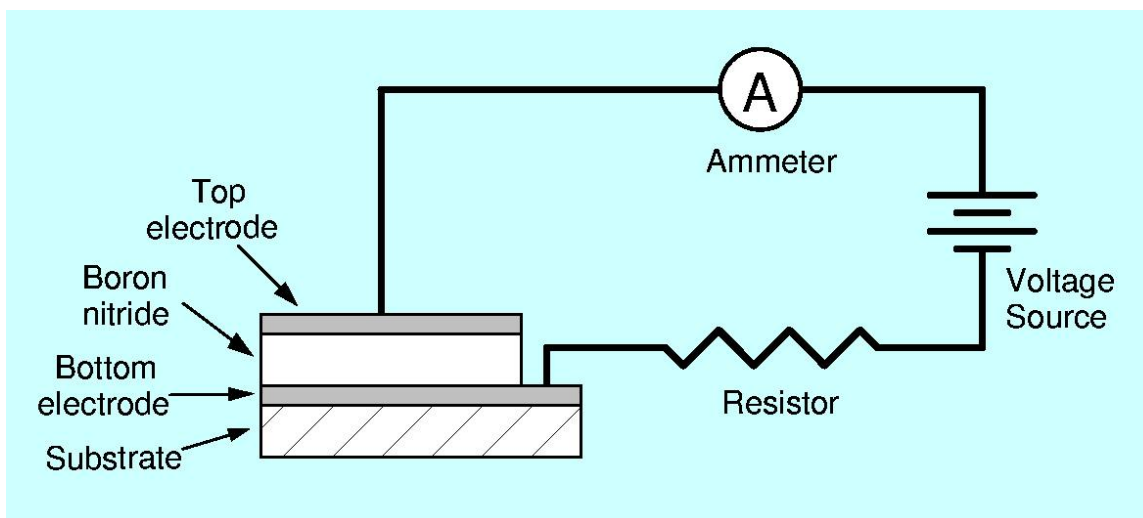
Figure 1. Steady-current FIND detection circuit.

For low neutron flux levels, the excess current is in the form of current pulses. In this case, a charge pulse amplifier circuit can be used to detect the pulses. The amplified pulses are then counted with a standard pulse counting instrument. For both measurement methods, the excess current is due to the free charge carriers produced by the interaction of thermal neutrons with the BN film in the detector element. The amplitude of a continuous excess current, or the count rate of charge pulses, is therefore proportional to the neutron flux at the detector. Details of the amplifier circuit, based on an Amptek® A250 preamplifier, are given in Appendix A.

MATERIALS PROPERTY REQUIREMENTS

Numerous issues must be considered in using solid BN for neutron detection, including the following:

- Charge carrier recombination and trapping (related to carrier mobility and lifetime)
- Neutron capture efficiency (related to ^{10}B content and BN thickness)
- Electrode contact resistance (relative to BN resistance)
- BN conductivity.

For the FIND device to work as a thermal neutron detector, the key BN materials properties of carrier mobility, carrier lifetime, and conductivity must meet the requirements described in the following subsections.

Charge Carrier Recombination and Trapping

The BN must be sufficiently defect-free for this type of detector to work effectively. Otherwise, the free carriers produced by the nuclear reaction will be trapped at defect sites before they can contribute fully to the current pulse induced [3,4] at the detector electrodes (that is, before they can reach the electrodes). By trapping or some other mechanism, the free electrons and holes generated as a consequence of the nuclear reaction of Equation (1) will recombine in an average time τ. Electron-hole recombination will be minimized if the carrier transit time τ_t through the material thickness is much less than this recombination time, or carrier lifetime, τ. For ohmic conduction, the transit time across the BN thickness d is equal to

$$\tau_t = \frac{d}{\mu E} = \frac{d^2}{\mu V}, \tag{2}$$

where μ is the carrier mobility, E is the applied electric field, and V is the voltage across the BN thickness.

The carrier lifetime and mobility are not well known for BN, and both likely depend on crystal phase, purity, carrier concentration, etc. Two crystal phases are of practical interest: hexagonal (hBN) and cubic (cBN). Of fundamental interest is the mobility-lifetime product $\mu\tau$, which is the average distance traveled by a free carrier, per unit electric field, before recombination or trapping occur. Recombination and trapping will not be a problem if $\tau \geq \tau_t$, or equivalently, if

$$\mu\tau \geq d^2/V . \tag{3}$$

For a practical working device, $\mu\tau$ should be several times the minimum value given by Equation (3).

Neutron Capture Efficiency

The BN thickness also directly influences the neutron capture efficiency. For example, to absorb 95% of normally incident thermal neutrons, a cBN detecting element would have to be about 460 μm thick (based on a BN density of 3.5 g/cm^3, a ^{10}B thermal neutron reaction cross section of 3837 barns, and the 19.6% abundance of ^{10}B in natural boron). Enriching the ^{10}B level to 100% (to obtain cubic ^{10}BN) would decrease the 95% absorption thickness to 94 μm. Depending on the values of μ and τ in BN, a thickness trade-off may exist between carrier lifetime and neutron capture efficiency.

Electrode Contact Resistance

The electrical contact between the BN detecting element and the electrodes must be conducting enough that the free carrier current generated by the nuclear reaction is not blocked from flowing in the external measurement circuit. If the resistance of the contacts is small compared to that of the BN film, then essentially all of the electric field produced will be across the BN, which is needed to sweep out any free charge. Such low resistance contacts are needed so that the potential applied between the top and bottom electrodes on the detecting element gives a voltage drop mainly across the BN and not across the BN/electrode interfaces. An ohmic contact (linear current–voltage characteristic) would ensure that this condition is met, and is preferable to a Schottky-barrier contact (non-linear current–voltage characteristic and typically higher contact resistance). The FIND device would

work with either type of contact, however, as long as the contact resistance is small compared to that of the BN film.

BN Conductivity

Another important consideration is the electrical conductivity or resistivity of BN. The material must be resistive enough that (1) the voltage difference between the detector electrodes required to attract the free carriers to the electrodes is on the order of a volt or higher, and (2) the background or dark current is low enough that it does not interfere with measurement of the signal current. This property will be determined by the BN crystal phase, purity, and morphology.

DETECTOR ELEMENT FORMS

Either a film or thin sheet of boron nitride may be used as the neutron-sensitive material in the FIND device. Two bulk forms of BN are readily available as thin sheets. One is polycrystalline, hexagonal-phase BN, typically formed from pressed powder. The purest such material readily available (>99.29% pure) is Combat® AX05 grade manufactured by Saint-Gobain Ceramics & Plastics, Inc. This bulk material has the drawbacks, compared to other forms of BN, of having small grain size and high porosity (reducing carrier lifetime), as well as poor mechanical strength (requiring thicker samples and thus higher bias voltages).

The other thin sheet form of BN is pyrolytic hexagonal-phase BN (pBN), available from the General Electric Advanced Ceramics Corporation. Pyrolytic BN is a freestanding sheet grown by high-temperature, low-pressure chemical vapor deposition. The graphite-like planes of pBN are highly oriented, parallel to the sample surface.

Films of either hBN (with, like pBN, a hexagonal structure analogous to graphite) or cBN (with a cubic structure analogous to diamond), deposited on a supporting substrate, can also be used in a FIND device. Such films can be produced using a number of film growth techniques, including various forms of physical and chemical deposition. The two phases have different densities, electrical resistivities, carrier mobilities, and growth habits. Based on these properties, one BN phase may be better suited for neutron detection than the other.

CARRIER LIFETIME AND MOBILITY CALCULATIONS

As discussed in the Charge Carrier Recombination and Trapping section, the BN film properties should be such that electrical carriers generated by the nuclear reaction of Equation (1) are able to reach the device electrodes (see Figure 1). The minimum value of the mobility-lifetime product $\mu\tau$ for which the FIND device will work as effectively as possible is that for which the carrier lifetime τ is equal to the carrier transit time τ_t across the BN film thickness. Based on this requirement, the minimum value of $\mu\tau$ can be calculated for a given active BN volume and acceptable dark current (which in turn depends on the BN resistivity ρ). This minimum value, as a function of ρ, is shown in Figure 2 for a 1-μm-thick BN film, 1 cm^2 in area, with a dark current of 1 nA.
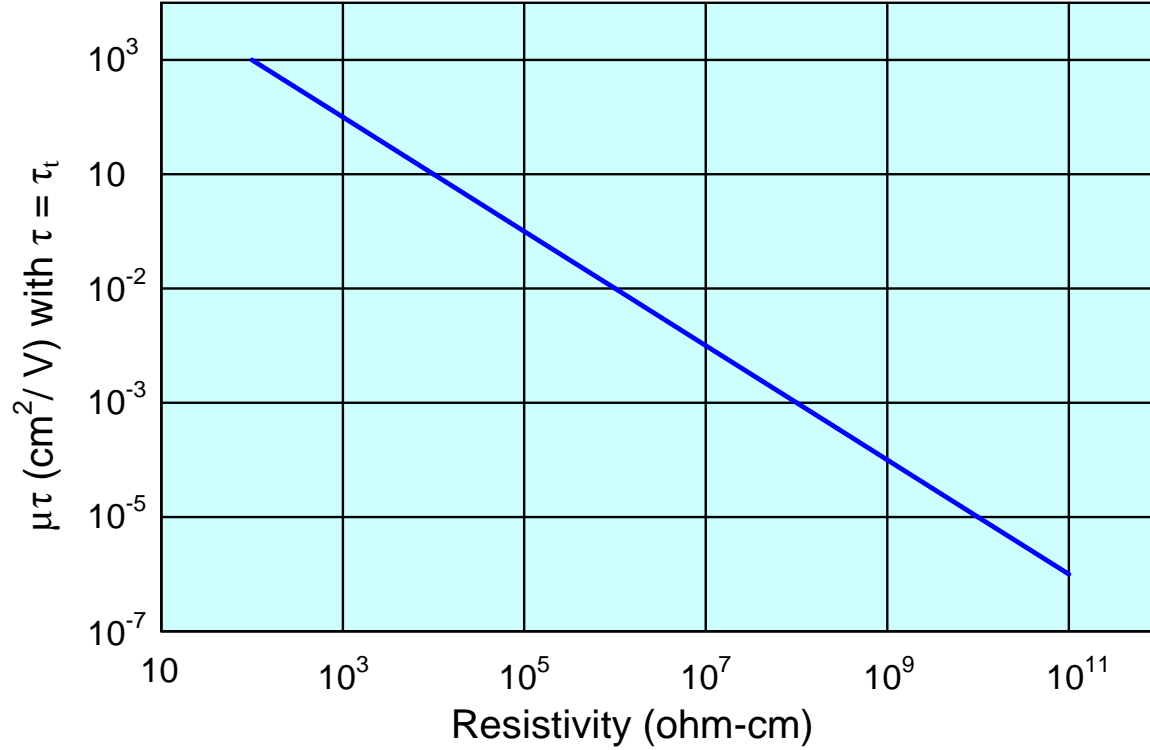
Figure 2. Minimum acceptable mobility-lifetime product versus BN film resistivity (with a dark current of 1 nA, film thickness d = 1 µm, and film area A = 1cm^2).

EXPECTED DETECTOR PERFORMANCE

Approximately 2×10^5 free carriers are generated in each reaction; see Equation (1). Assuming no $\mu\tau$ limitations (that is, Equation (3) is satisfied), the expected amplitude V_p of an output pulse from the Amptek® A250 charge sensitive preamplifier (with a sensitivity of 0.16 µV/electron) is either 32 mV (when both the free electrons and holes reach the device electrodes or 16 mV (when only electrons or only holes reach one of the device electrodes). In general, V_p will depend on the relative values of the electron and hole mobilities and lifetimes in BN. For a given reaction, V_p will depend on the thickness of the BN and the exact location of the reaction within the BN.

The mean free path x of a free charge carrier in BN is given by

$$x = v\,\tau$$

$$= \mu\,E\,\tau \qquad (4)$$

$$x = \frac{\mu\,\tau\,V}{d}\ ,$$

where v is the carrier drift velocity reached in the applied electric field E (produced by the application of voltage difference V across BN thickness d).[*] The total charge collection distance is 2x.

---

[*] Here, $\mu\tau$ represents an average of the mobility-lifetime products for free electrons and holes. That is, $\mu\tau = \left(\mu_e\tau_e + \mu_h\tau_h\right)/2$. If $\tau = \tau_e = \tau_h$, then $\mu = \left(\mu_e + \mu_h\right)/2$ represents the average mobility of electrons and holes.

6

The Hecht equation[5] describes the charge collection effieciency in terms of the carrier mean free path, the detector thickness, and the distance from the reaction point to each detector electrode.[6] In the limit that these reaction point distances are much greater than the carrier mean free path,[*] the charge collection efficiency ζ is given by (see Equation (4))

$$
\zeta = \begin{cases} 2\mu\tau V/d^2 & (\mu\tau V/d < 1) \\ 1 & (\mu\tau V/d \geq 1). \end{cases}
\tag{5}
$$

The upper expression of Equation (5) applies when charge collection at the device electrodes is "$\mu\tau$ limited" as given by the inequality in parentheses. The detector sensitivity S can then be expressed in terms of the BN material properties n_B, σ_B, μ, and τ, and the detector parameters A, V, and d: [†]

$$
S = (2\, n_B \sigma_B\, \mu\tau) \cdot \left(\frac{AV}{d} \right),
\tag{6}
$$

where n_B is the boron atom number density, σ_B is the effective thermal neutron cross section of boron in natural BN, and A is the detector active area. Note that the first quantity in parentheses in Equation (6) contains only material property parameters, while the second quantity contains only experimental parameters (detector geometry and applied voltage).

The expected measured nuclear reaction rate ν (count rate) for a FIND device is given by

$$
\nu = \left(1 - e^{-\zeta\sigma_m d}\right) \cdot \Phi A
$$
$$
\nu \approx \zeta \Sigma \Phi \qquad (\zeta\sigma_m d \ll 1),
\tag{7}
$$

where $\left(1 - e^{-\zeta\sigma_m d}\right)$ is the fraction of thermal neutrons "absorbed" by a sample of thickness d and area A, Σ is the total sample cross section for thermal neutrons, σ_m is the total cross section for thermal neutrons per unit volume, and Φ is the thermal neutron flux.

---

[*] In this limit of the Hecht equation, the charge collection efficiency is $2x/d$ for $2x \leq d$.

[†] Note that if $\mu_e\tau_e \gg \mu_h\tau_h$, for example, then $S = (n_B\sigma_B\,\mu_e\tau_e) \cdot (AV/d)$.

APPROACH AND METHODS

BN FILM GROWTH AND CHARACTERIZATION

The BN films were deposited at UMich by magnetron sputtering of an hBN target in an ultra-high vacuum (UHV) chamber. Energetic nitrogen ions generated by a Tectra Electron Cyclotron Resonance (ECR) source were directed at the growing films. The ion energy was controlled by a DC bias applied to the substrate. This bias voltage is crucial in determining if the BN films are grown in the hexagonal phase or in the cubic phase. A reduced bias growth process is used to reduce the residual stress of cBN films.[7] The substrates used for this research were single crystal (100) Si. The substrate temperature during film growth was typically 1000°C. The growth chamber is shown schematically in Figure 3.
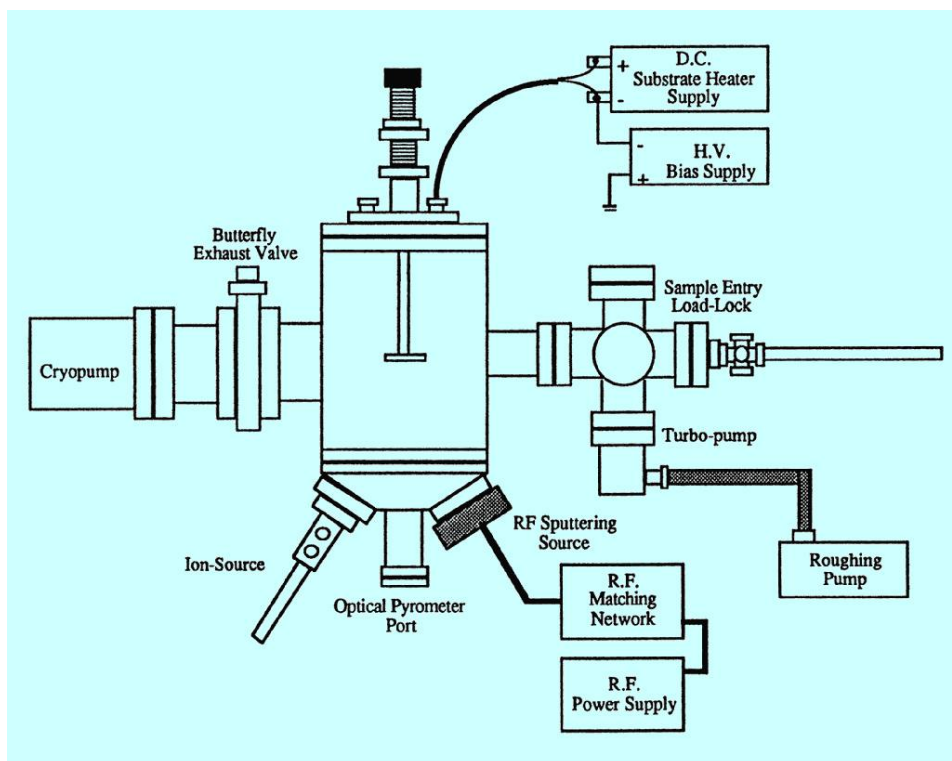
Figure 3. UHV BN film growth chamber at UMich.

To optimize the BN film growth process with respect to growth rate and reproducibility, an *in situ*, real-time optical film growth monitor[*] was installed in the growth chamber illustrated in Figure 3. The principle behind this instrument is the measurement of the sample's real-time reflectivity of a blue laser beam (410 nm wavelength). The resulting reflected intensity versus time curve exhibits oscillations as the BN film thickness corresponds to either a constructive interference condition (curve maximum) or a destructive interference condition (curve minimum). The curve can be used to extract the instantaneous thickness of the film, its optical constants (n and k), and the rate of increase of the film thickness.

---

[*] RateRat Pro, developed and manufactured by k-Space Associates, Inc., Ann Arbor, MI.

The film thickness d is calculated from the constructive interference condition

$$2d = m\lambda/n \ , \tag{8}$$

where m is an integer (m = 1 in this case), n is the refractive index of the BN film (~ 2.3), and λ is the wavelength of the light. Note that $n < n_{Si}$ ($n_{Si} \approx 3.9$ for blue light), and so no phase shift exists at the film-silicon interface. Using a blue laser provides a more sensitive measure of the optical properties because the interference fringes are more closely spaced (in time or film thickness) for the shorter wavelength compared to a more conventional red diode laser probe.

The crystal phase composition of the films was characterized with Fourier transform infrared (FTIR) spectroscopy. A scanning electron microscope (SEM) was used to examine film morphology.

CARRIER LIFETIME MEASUREMENT METHODS

The time-resolved reflectivity (TRR) method, shown schematically in Figure 4, can be used to measure very short carrier lifetimes. In the TRR (or pump-probe) method, the intensity of a laser beam reflected from the sample surface is measured as a function of time. This time-resolved intensity is proportional to the free charge carrier density at the sample surface, enabling determination of the carrier lifetime using the type of analysis shown in Figure 5.

The decay time is determined by observing the time dependence of the reflected light intensity immediately following the sample excitation,[8] as illustrated in Figure 5. In the figure, the carrier density in the sample increases from n_o to $(n_o + \tau G)$ when irradiated with light of frequency ν. When the light is turned off at t = 0, the carrier density decays back to its "dark" value with a characteristic decay time defined as the carrier lifetime τ. The generation rate of carriers during photoexcitation is given by the constant G. The carrier lifetime τ is determined from the initial (linear) part of the decay curve, where $n(t) \approx n_o + \tau G[1 - (t/\tau)]$, in which case, $n = n_o$ when t = τ.

In the implementation of the TRR method used initially,[2] a pulsed titanium-sapphire laser with a repetition rate of 82 MHz and a pulse width of 40 fs provides a pulsed laser beam that is split into pump and probe beams in a 10:1 intensity ratio, respectively. Figure 4 shows the optics needed to bring the pump and probe laser beams into spatial and temporal coincidence at the sample surface. Both beams are focused onto the sample with respective spot diameters of 100 and 50 μm. The pump beam is s-polarized while the probe is p-polarized. The pump and the probe beams are modulated with a photoelastic modulator at 50 kHz, and a mechanical chopper at 60 Hz, respectively. The reflectivity signal is measured by a lock-in amplifier/photodiode combination. The probe beam is delayed with respect to the pump beam with a translation stage delay rail, which has a 0 to 600 ps delay range. The time-resolution of the measurement is approximately 200 fs.
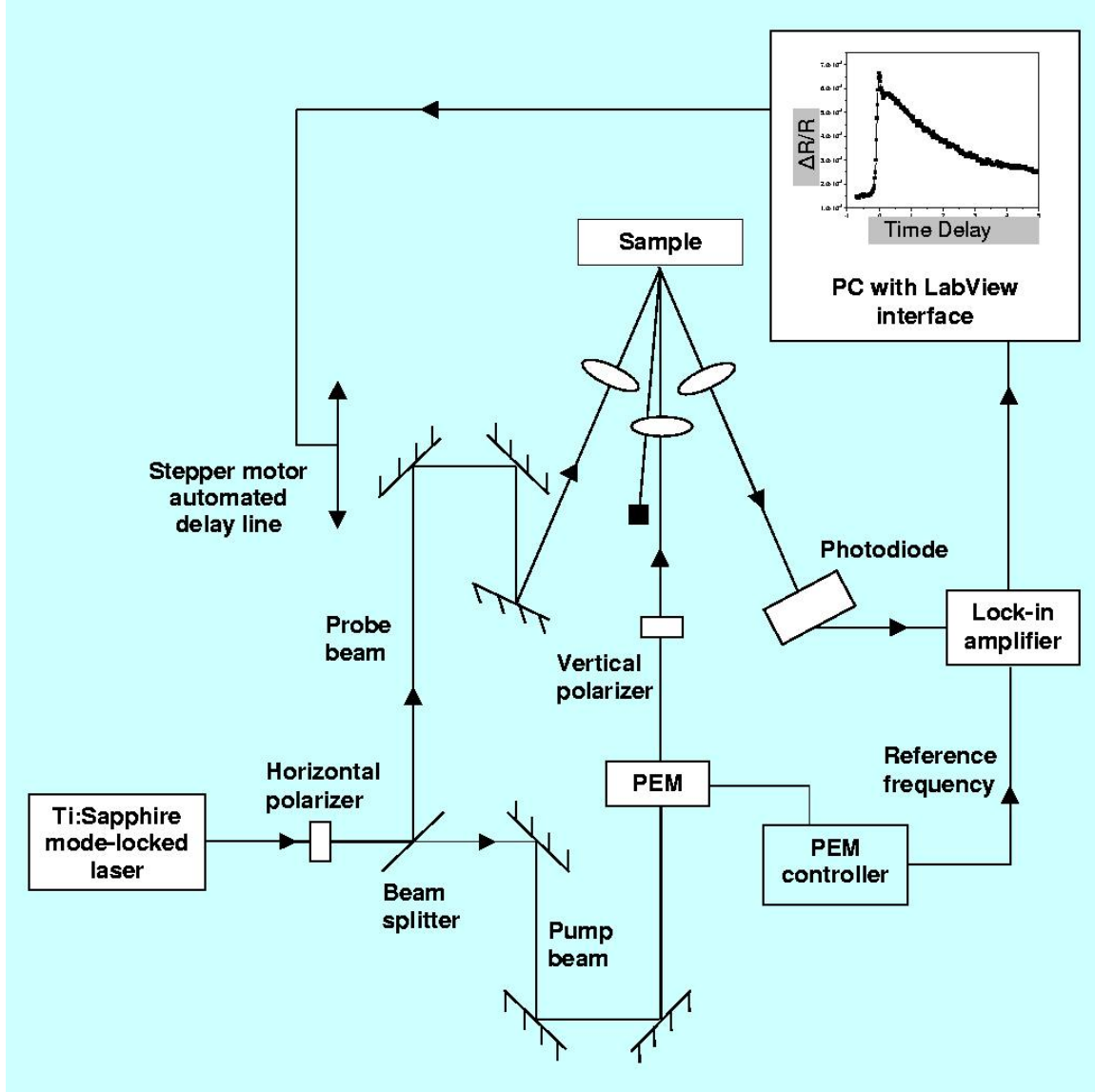
Figure 4. Single-laser, ultra-fast, time-resolved reflectivity (TRR) system.

In the experimental setup described above, the use of a mechanical delay rail imposes a maximum measurable value of the carrier lifetime of about 500 ps. This shortcoming of the TRR method can be overcome by using two lasers to provide the pump and probe beams, instead of splitting, delaying, and then recombining the beam of a single laser. The phase delay between two lasers can be electronically, rather than mechanically, synchronized. Highly stable power output is required, however, because of the need to repeatedly scan the sample for hours to improve the signal-to-noise ratio. Dual ultra-stable Er-doped fiber lasers with the required phase-locking electronics were procured from Menlo Systems GmbH for this purpose. The short pulse width (< 100 fs) and long delay times (up to 10 ns) of the dual fiber laser system enable a highly precise measurement of the carrier lifetime. A diagram of the pump-probe set-up for the dual fiber laser system is shown in Figure 6.

$$n(t) = n_o + \tau\, G\, e^{-t/\tau}$$
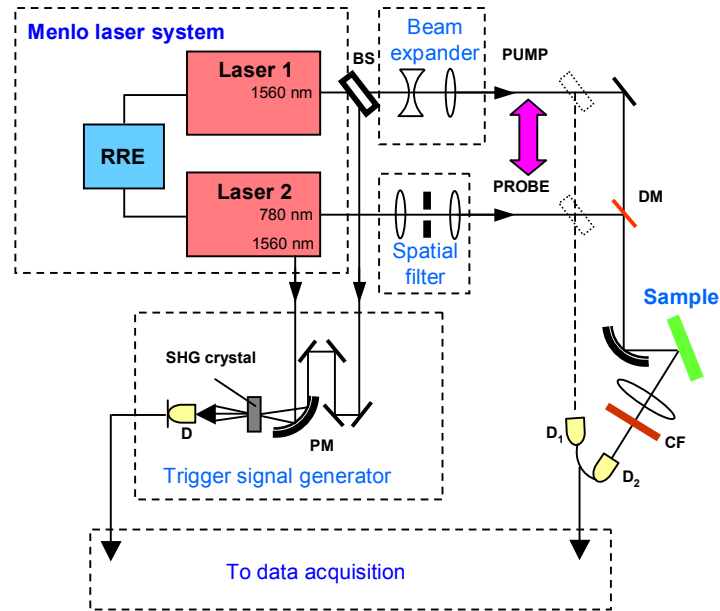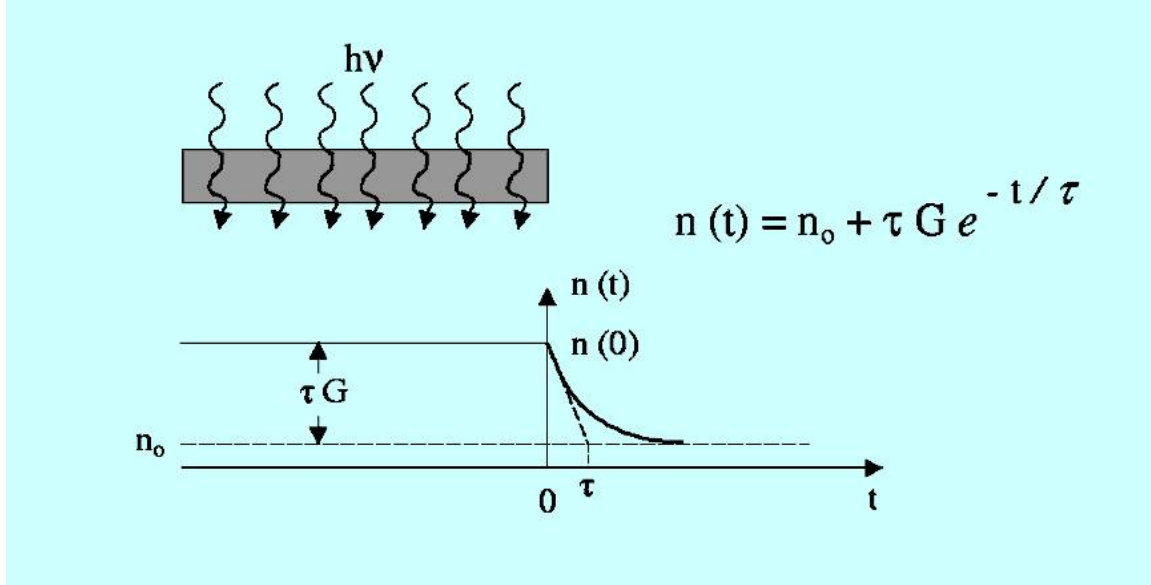
Figure 6. Dual fiber laser ultra-fast TRR system.

    Delivery of the dual fiber laser system was not made until early January 2007, more than 5 months after the project started. In the meantime, an ultra-fast photon correlation fluorescence technique was used to measure the BN carrier lifetime. This method is based on the fact that photo-excited carriers will recombine (or become re-trapped), emitting optical fluorescence, after some characteristic recombination time, or lifetime. The carrier lifetime can be obtained by measuring the time required for this fluorescence to appear. The carriers are excited by a very short (20 fs) laser pulse generated by a titanium-sapphire laser oscillator operating at 80 MHz at a fundamental wavelength of 800 nm.

The laser pulse triggers a photon counting detector (a fast diode) that then marks the arrival time of fluorescence photons. When a fluorescence photon is detected, the time interval between its arrival and the laser clock trigger signal is recorded and binned to a multi-channel analyzer (MCA). The photon counter is then reset and the timing process is repeated. The resulting MCA histogram reveals the decay of the photoluminescence signal caused by recombination/trapping of photo-excited carriers. The 80 MHz repetition rate of the laser pulse permits measurements over a 12.5 ns time scale, and the MCA resolution (4096 channels) corresponds to a time resolution of 12.2 ps. Note that pump-probe reflectivity measurements may be more sensitive than those obtained by the fluorescence technique because not all carrier recombination processes will be radiative.

CARRIER MOBILITY MEASUREMENT METHODS

Because of the difficulty in measuring the Hall mobility of highly insulating samples, a corona discharge method for determining the carrier drift mobility of BN from the time decay of a surface voltage was investigated. In this technique, the sample is prepared with a grounded metallic electrode on its bottom surface (see Figure 7). A high voltage (around 3 to 8 kV) is applied, relative to ground, to a needle-shaped electrode positioned a few centimeters above the free surface of the film (i.e., the non-electroded surface). The film's free surface is also surrounded by a grounded flat metal shield. The high voltage produces a so-called corona discharge (a plasma consisting of electrons and ionized air or water molecules) at the tip of the needle. The ions follow the electric field lines to the metal shield and to the film's free surface. Charge accumulates on the film surface, thus producing a potential difference, V, between the surface and the grounded back side of the film that builds up with time. An electron (or hole) current I flows through the film sample thickness because of this potential difference and neutralizes the arriving ions. In the steady state, the sample current I_o is equal to the current arriving at the surface from the corona discharge, and the surface voltage reaches a steady-state value V_o.

If the discharge is turned off, the surface potential will decay with time from this steady-state value. Under space-charge-limited[9] (SCL) constant-current conditions, the build-up or decay of surface voltage V has been shown to depend in a simple way on the sample thickness and carrier drift mobility μ.[10,11] The mobility can be determined from the build-up or decay of the surface voltage with time, or from the steady-state value V_o (if the sample dielectric constant and dimensions are known). The SCL steady-state sample current will be related to the steady state surface voltage by[12]

$$I_o = \frac{9}{8} \epsilon \mu \frac{V_o{}^2 A}{d^3} \ ,$$

(9)

where $\epsilon = Cd/(\epsilon_o A)$ is the boron nitride dielectric constant, C is the sample capacitance, and ϵ_o is the permittivity of free space. The carrier mobility of a trap-free insulator under SCL steady-state conditions is then given by

$$\mu = \frac{8}{9} \frac{I_o d^2}{C V_o^2} \ .$$

(10)
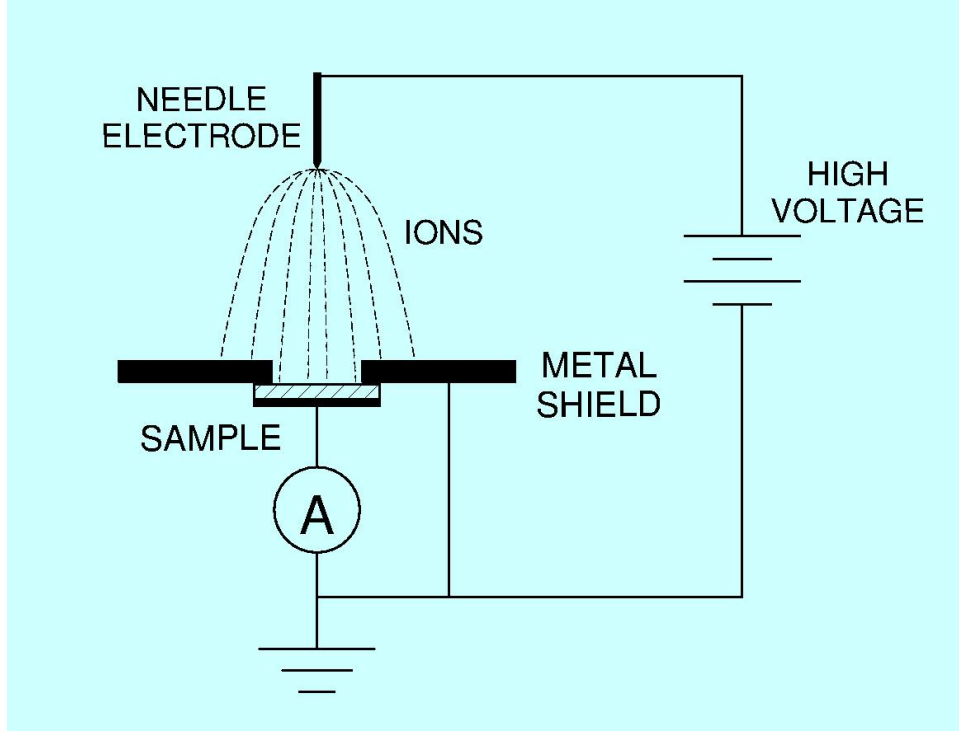
Figure 7. Corona discharge surface voltage measurement method.

For insulators with traps, the mobility of Equation (10) represents an effective or trap-modulated mobility.[10] The transit time τ_t of charge carriers across the sample thickness, d, under SCL conditions is given by[10]

$$\tau_t = d\sqrt{\frac{2C}{I_o\mu}} \; . \tag{11}$$

This transit time is also approximately the time needed to reach steady-state conditions.

In the absence of SCL conditions, the current will be related to the voltage by Ohm's law,

$$I = n\,e\,\mu\,\frac{VA}{d} \; , \tag{12}$$

where n is the carrier density and e is the electron charge. Ohmic current–voltage characteristics can also be observed when surface conduction (leakage current) around the sample edge dominates bulk conduction through the sample.[13]

A drawing of the corona triode apparatus used for the carrier mobility measurements is shown in Figure 8. One requirement for this mobility measurement method is the application of high voltage both to the corona point and the corona triode grid while maintaining the corona and sample currents constant (when determining mobility from surface voltage build-up or decay). To meet this need using standard constant-voltage, high-voltage power supplies, special feedback circuits were developed to control and measure these currents (see Appendix B). The special circuit for maintaining a constant sample current is not needed for measurements based on steady-state conditions, although

the sample current and voltage must still be measured. The feedback circuit for keeping the corona current constant in this case is still required, however, because the sample surface voltage is determined by measuring the change in grid voltage for a given current going to ground, with and without a sample in place. The corona current incident on the triode grid must the same in both instances to obtain meaningful results.
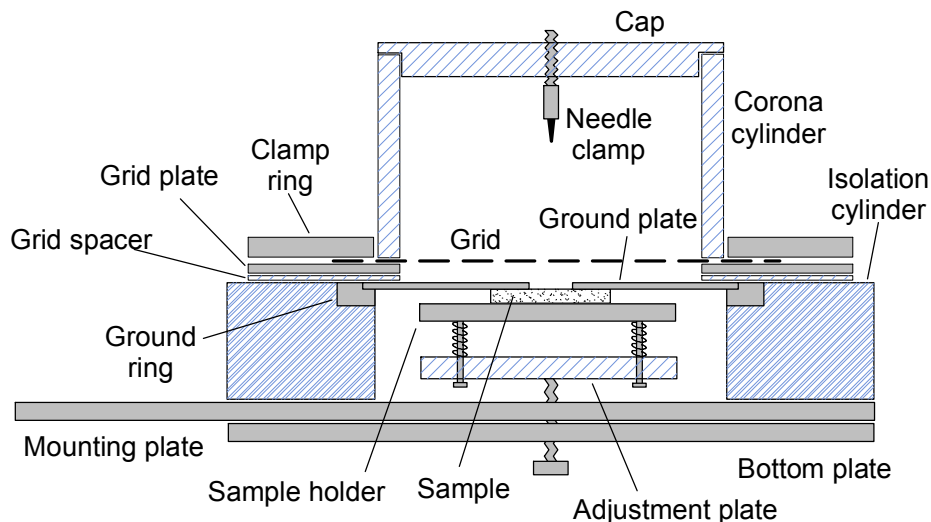
Figure 8. Corona triode apparatus (cut-away side view).

ELECTRODE AND FIND DEVICE PREPARATION

Electrode Preparation

One type of conducting electrode for the FIND device (see Figure 1) consists of multilayer metal films deposited using the SSC San Diego UHV ion beam sputtering system shown schematically in Figure 9 (only two of the three Kaufman sputter ion sources are shown). The boron nitride electrical contact method used here is similar to that developed at SSC San Diego to make contact to semiconducting diamond.[14] For the present case, titanium (Ti) metal (followed by diffusion barrier and contacting layers) is used to coat BN, and the sample is then heated in an inert-atmosphere. Ti reacts with BN to form titanium nitride (TiN) and titanium borides, both of which are conducting. A barrier layer of tungsten (W) or TiN prevents formation of titanium oxides (during atmospheric transfer of the samples) and their subsequent diffusion through a gold (Au) or silver (Ag) contacting layer (to which wire bonds may be formed).

Another type of front side electrode used was a single layer (~ 50 nm thick) of sputtered gold. Note that for a FIND device, freestanding BN sheets require both front and backside metal electrodes deposited on the BN, whereas films need only a front-side metal contact on the BN (the Si substrate serves as the backside electrode).

Good electrical contact to the backside of the Si substrates of the BN film samples, needed for carrier mobility measurements (using the corona triode apparatus) and configuration as a FIND device, was made in one of two ways. Some samples had a platinum (Pt) backside contact (annealed at the film deposition temperature) that provided an ohmic contact. Other samples had no Pt coating

(or it had been removed). In that case, ohmic contacts were formed by coating the backside of the Si substrate with Al, with a subsequent 480°C, 30-minute anneal in flowing argon (Ar) gas.
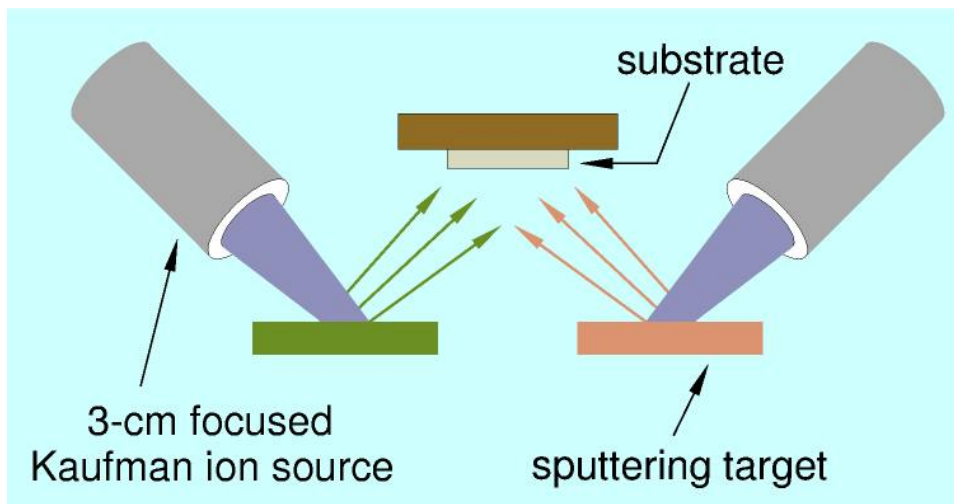

Figure 9. UHV ion beam sputtering system.

FIND Device Configuration

Front and backside multi-layer Ag/W/Ti contacts were ion beam sputter deposited onto a pBN sample (SSC San Diego sample BLK23) to prepare it as a FIND device. The front-side contact was wet-etch patterned[2] (as a 5 mm × 5 mm square) to isolate the contact from the sample edge. This method ensures that surface currents do not flow around the edge from the front to the back contact when a bias voltage is applied between the two contacts. The sample was then attached to a sapphire substrate, using silver paint to connect silver wires to the electrodes, and annealed in flowing Ar gas at 700, 800, and finally 900°C to react the Ti electrode with the BN. The lower temperature was suggested by previous measurements that showed a minimum in the resistance between interdigitized electrodes on the surface of a similar sample after annealing at that temperature (see Figure 37 and associated discussion). Observation of a post-anneal, gray-colored contamination layer (perhaps from the silver paint) on the exposed BN surface (surrounding the top electrode) might explain the previous result. Anneals at higher temperature lightened the contamination layer color, but did not completely eliminate the layer. After the final anneal, the contamination layer was scraped away, leaving a fresh BN border around the top electrode. The silver wires of the electroded sample were then indium soldered to an empty dip socket to form a FIND device for testing.

Hexagonal BN film sample OUT111 (UMich sample 013006, 250 nm thick, ~ 1.2 cm square), with a favorable carrier lifetime of about 3 ns (see the CARRIER LIFETIME MEASUREMENT RESULTS section), was mounted as a FIND device by applying a sputtered Au electrode (~ 50 nm thick, ~ 6 mm × 6 mm area) to the film surface and attaching a contact wire to this electrode with silver paint (see Figure 10). The doped Si (100) wafer, with conductivity in the range of 2 to 10 Ω-cm, served as the bottom electrode for the device. With this electrode configuration, an electric field can be applied normal to the plane of the BN film. Electrical resistance measurements were made using an ohmmeter (see the ELECTRICAL PROPERTIES section).
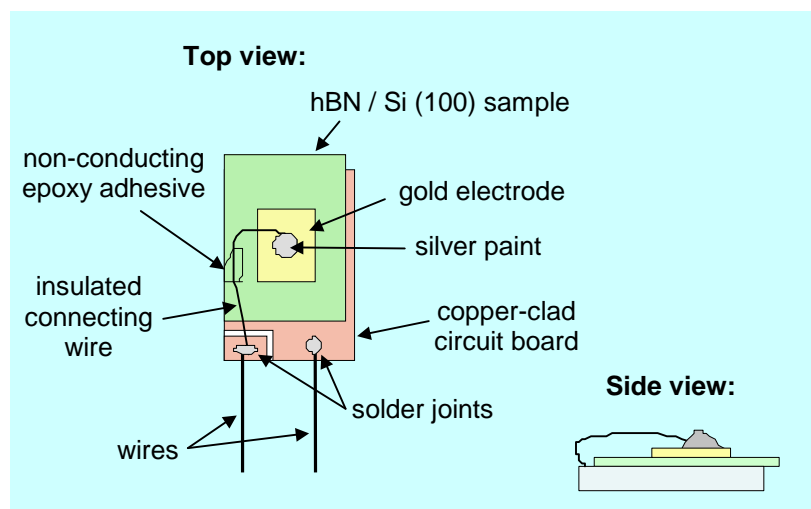
Figure 10. Hexagonal boron nitride (hBN) film on Si configured as a FIND device.

ELECTRICAL PROPERTIES CHARACTERIZATION

The current–voltage properties of various BN samples and their patterned electrodes (see the Electrode Preparation section) were measured using standard techniques.[2] Fine silver, copper, or nickel (Ni) wires were attached to the patterned electrodes using silver paint. Some electrical measurements were made *in situ* as a function of temperature in a tube furnace in flowing Ar gas.

THERMAL NEUTRON DETECTION METHODS

Single FIND Device

The detecting element of the FIND device consists of a thin sheet or film of BN sandwiched between conducting electrode layers (that is, a capacitor structure). The electric field within the BN, produced by the voltage applied across the device electrodes, collects any free charge generated by the nuclear reaction of Equation (1) that reaches the electrodes without being trapped or undergoing recombination. Each nuclear event will therefore cause a sudden increase in the charge residing on the device electrodes. For low neutron flux densities, each increase will be discernable as a distinct charge pulse. A charge-sensitive amplifier converts this charge pulse into a voltage pulse for subsequent display and processing.[15] The nuclear reaction rate is measured by counting the voltage pulses from the charge-sensitive preamplifier.

Improvements were made in a previously built charge pulse amplifier circuit[2] based on an Amptek® A250 charge pulse preamplifier (see Appendix A). This circuit detects the current pulses produced when thermal neutrons react with ^{10}B in the FIND device.

Alternative Detector Devices using BN

An alternative configuration for a BN-based thermal neutron detector consists of a diode structure that operates in a reverse-bias regime. In this regime, the majority carriers resulting from impurities in the material are blocked by the junction barrier. A neutron reaction event will generate a burst of minority carriers. The electric field across the junction will cause these carriers to be collected at the

device electrodes, producing a current pulse (measured as described above in the Single FIND Device section).

Two diode structures potentially have a high intrinsic detector efficiency (the fraction of incident neutrons that trigger an event detectable at the electrodes). Both structures use a thick BN layer for neutron capture. The first type is a so-called p-i-n structure that contains three semiconducting regions, each with a different doping level: a p-doped region, an intrinsic region, and an n-doped region. The intrinsic region is for neutron detection, and must be as thick as possible to maximize the device efficiency. Since the carrier lifetime in the intrinsic region is, in general, significantly higher than that of the doped regions, this layer not only serves as the neutron capture area, but also provides a high probability for capture of the free carriers produced by the neutron reaction. While the intrinsic region must be BN, the other two regions can be made from any doped semiconductor (such as silicon). The second type of diode structure is a deep depletion p-n diode in which at least the deep depletion region consists of BN. Again, the thickness of the deeply depleted layer should be as large as possible so that a large fraction of the incident neutrons are captured.

The samples to be tested will consist of arrays of microfabricated diodes with a cBN active region (a few microns thick) deposited on a Si (100) wafer. A contact layer of Ni (~ 200 nm thick) will be deposited using DC sputtering. To facilitate wire bonding, an additional layer of Au (~ 200 nm thick) will be deposited on top of the Ni layer.

Testing of these alternative detector devices is to be carried out at the Intense Pulsed Neutron Source (IPNS) at Argonne National Laboratory, a general user facility with access to neutron beams ranging in energy from 0.1 meV to 1 eV. This energy range spans the sub-thermal to supra-thermal energies typical of the output from an accelerator-based neutron source. A monochromatic beam flux of approximately 10^5 neutrons per second is typical for the IPNS source. A conventional boron trifluoride gas proportional counter detector will serve to calibrate the neutron flux seen by the BN diode detectors.

Multiple FIND Devices and Directional Capability

A detector to determine the incident direction of thermal neutrons can be formed from three orthogonal pairs of planar BN detector elements (FIND or BN-diode devices), as shown in Figure 11. For illustration purposes, each pair is a different shade in the figure, and the cube halves are offset so that the opposing elements are visible. An SSC San Diego invention disclosure has been submitted for an omnidirectional thermal neutron detector based on this concept.[16] This detector might take the form of a cube, or cube corner, for example. Each opposing side of the cube configuration consists of a planar BN detector element. Together, the two opposing sides of the cube form a detector element pair (one of three orthogonal pairs), as shown in Figure 11.
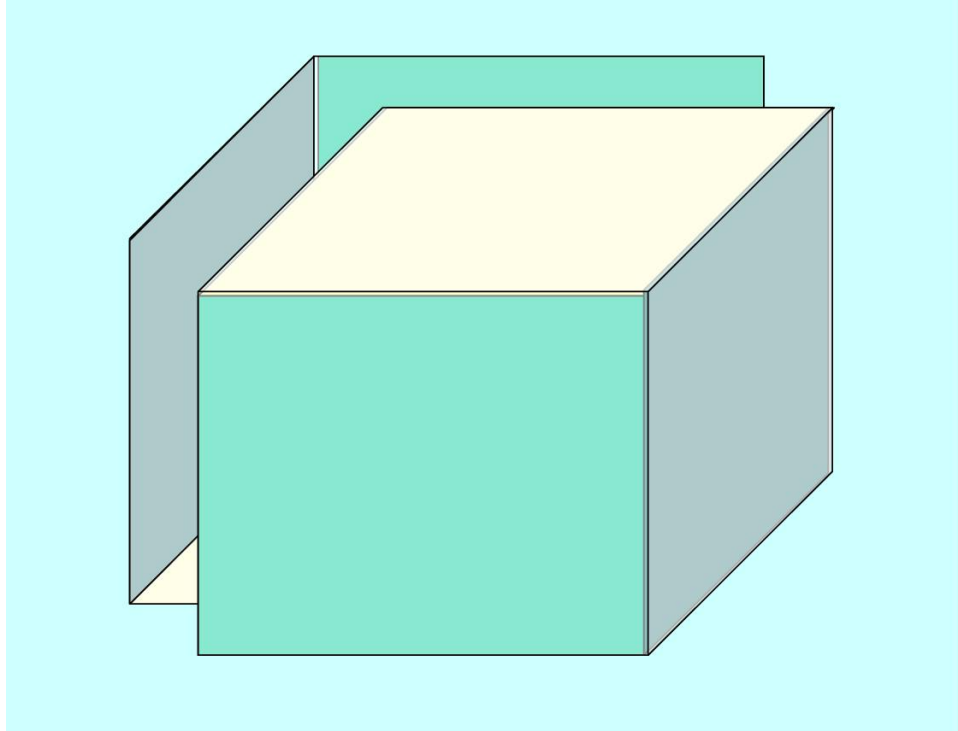
Figure 11. Three pairs of BN planar detector elements.

By measuring and comparing the thermal neutron detection count rate for each of the six detection elements, the direction (in three-dimensional space) of the neutron flux incident on the detector can be determined. An example, looking edge-on at one pair of parallel planar detector elements (each opaque to the transmission of thermal neutrons for illustration purposes), is shown in Figure 12. The relative count rate (black numbers) is shown as a function of the neutron flux incident angle.

Figure 12. Relative count rate of opposed detector elements (blue).

The size of a "FIND cube" relative to that of a conventional ^{3}He tube (gas proportional counter), each with the same sensitivity (13 cps/nv), is shown in Figure 13.

Figure 13. Relative size of a "FIND cube" omnidirectional detector and a ^{3}He tube.

RESULTS

BORON NITRIDE FILM GROWTH AND STRUCTURAL CHARACTERIZATION

Film Growth and Thickness Monitoring

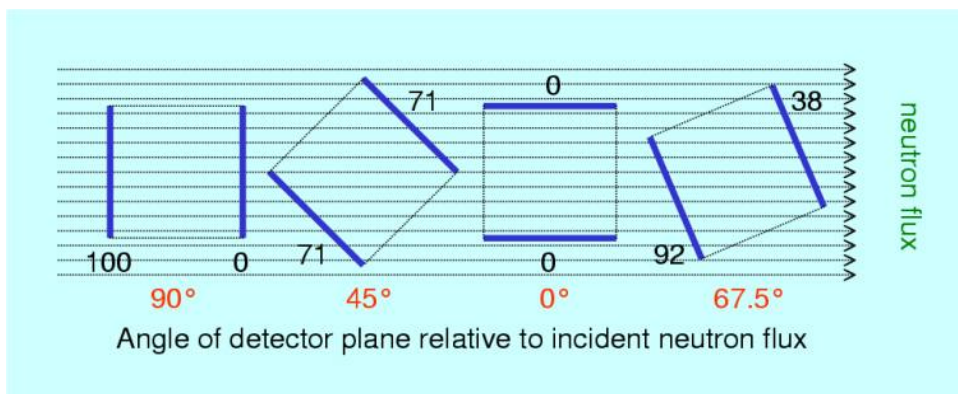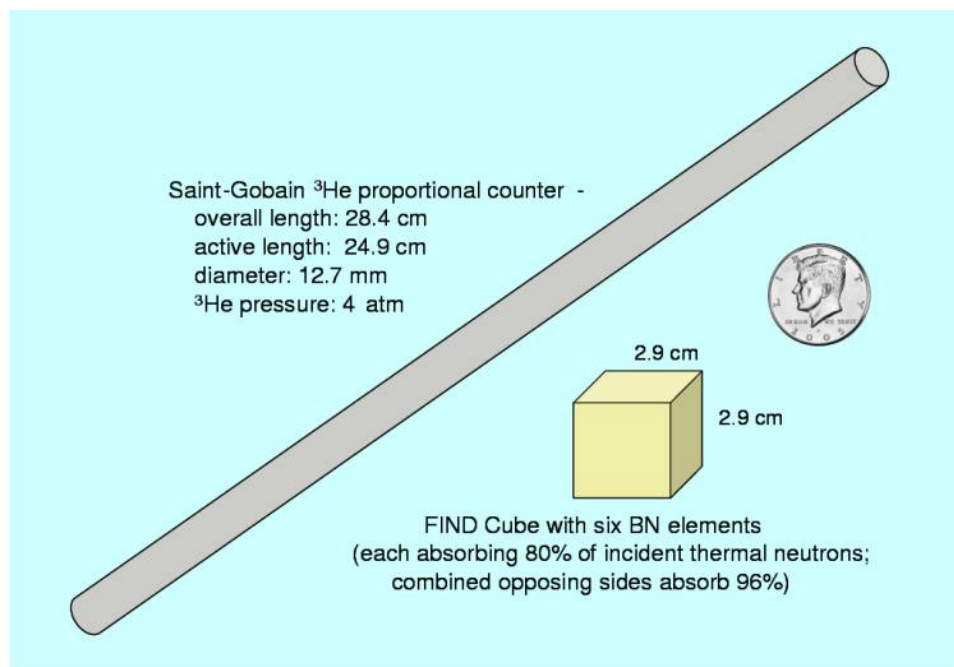The screen shot of Figure 14 shows the time dependence of the reflectivity of UMich cBN film sample 050407 during the 5.5 hour growth process. The reflectivity was measured real-time using the blue laser film growth monitor described in the BN FILM GROWTH AND CHARACTERIZATION section. The 100-nm-thick film was deposited on (100) Si. The growth conditions for this film were: substrate temperature = 1000°C, pressure = 3 mTorr, nitrogen gas (N$_2$) flow = 5 sccm, Ar flow = 5 sccm, substrate bias = -120 V, and RF power = 250 W. The reflectivity curve is fit in real time to a sinusoidal function that represents the interference of the beam reflected from the top surface of the film with the beam reflected from the top surface of the silicon substrate.
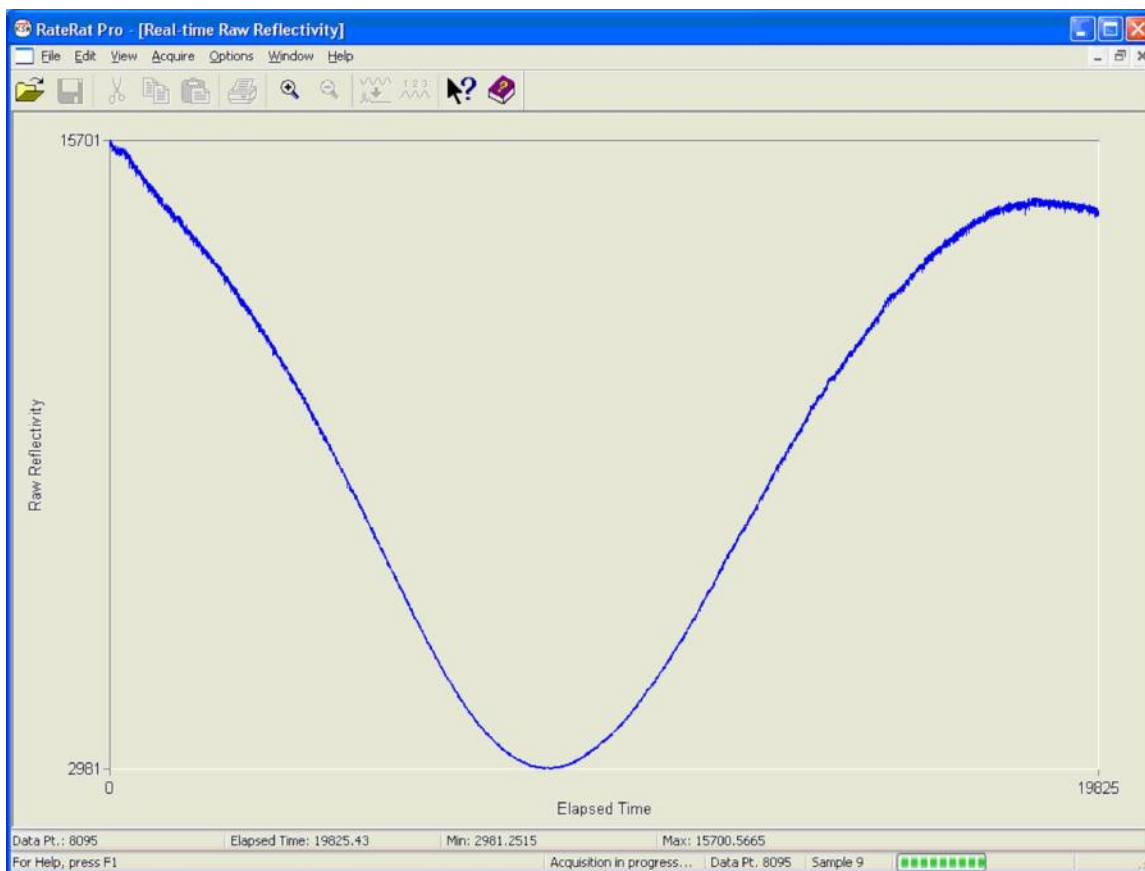
Figure 14. Real-time reflectivity during growth of a cubic boron nitride (cBN) film.

Some previously deposited cBN films with thicknesses of 100 to 200 nm were too thin to suppress electrical leakage (perhaps because of pin holes) when a bias was applied between the Si substrate and a metal electrode deposited on top of the film surface. Compared to thicker films, these thin films have a larger capacitance, which is an undesirable condition for the charge pulse amplifier detection circuitry. To address these two issues (leakage and capacitance), the growth of thicker films (on the order of 500 to 1000 nm) was pursued.

Figure 15 shows the real-time reflectivity trace obtained during the continued growth of UMich cBN film sample 050407 over a period of approximately 20 hours. Five orders of constructive interference were observed, corresponding to a thickness of 233 nm according to Equation (8). The overall decay in the reflectivity amplitude is caused by a combination of increasing surface roughness and bowing of the substrate because of stress in the film. Growth was continued for 6.7 hours more until the sample had a total thickness of 314 nm. The growth conditions for this sample were: time = 26.7 h, substrate temperature = 1050°C, substrate bias = -120 V, pressure = 3.0 mTorr, N_2 flow = 5 sccm, Ar flow = 5 sccm, RF power = 250 W, and sputter target DC bias ≈ -1030 V.
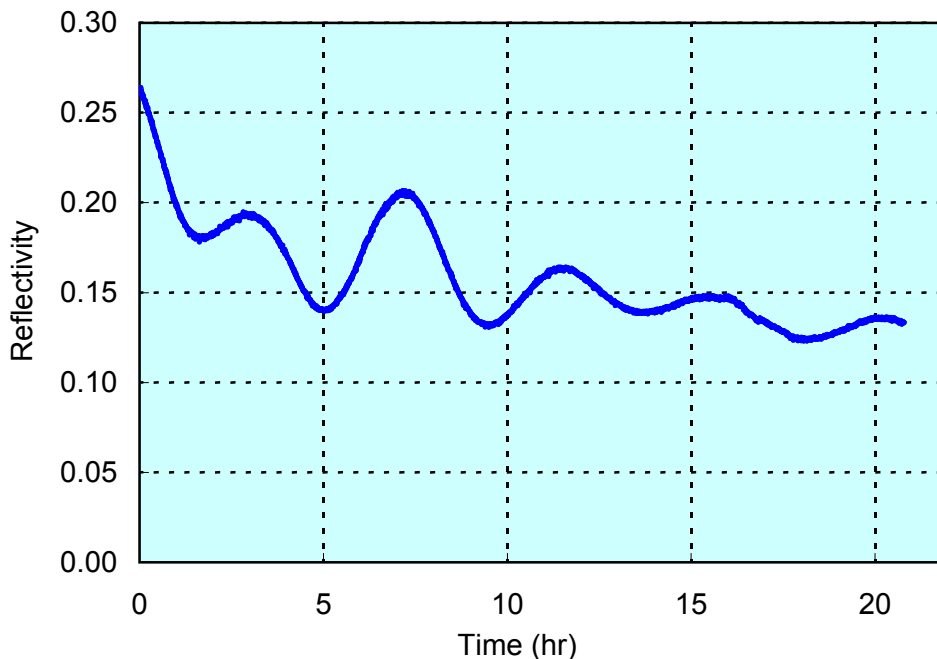

Figure 15. Reflectivity versus total growth time for a 233-nm-thick cBN film.

Having established a base-line for the cBN film growth parameters, the next step was to grow a much thicker sample, this time using the "reduced bias" technique.[7] In this method, growth is initiated at a somewhat higher substrate bias (-150 V) to ensure nucleation of the desired cubic phase, and then the bias is reduced to -120 V. Figure 16 shows the FTIR spectrum of UMich sample 051907 grown under reduced bias conditions. The presence of a single absorption peak at ~ 1075 cm^{-1}, attributable to a transverse optical (TO) vibrational mode, confirms that this film is single-phase cubic BN. Based on the growth rate of the sample of Figure 15 (grown without using the reduced bias technique), the total thickness of the Figure 16 sample is estimated to be at least 557 nm.

According to previous experience with the reduced bias technique,[7,17] additional improvement in growth rate by a factor of 5 to 6 is expected if the bias is further reduced to about -60 V, as suggested by Figure 17 (figure from Litvinov and Clarke [7,*]). The figure inset shows the increase in growth rate as the substrate bias is reduced.
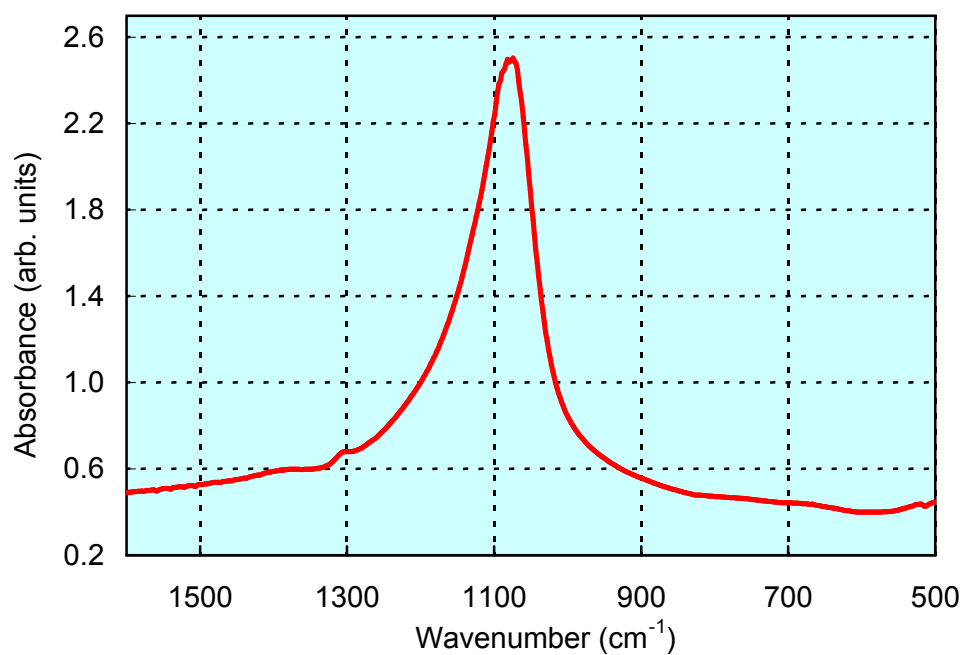

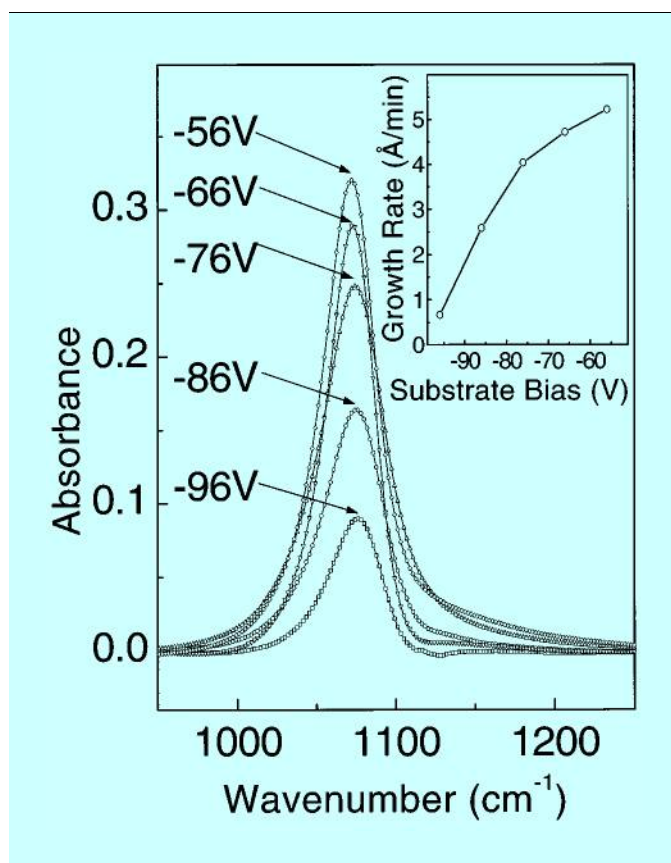Figure 16. FTIR spectrum of BN film with single TO mode, expected for cubic phase.

Figure 17. FTIR spectra for cBN films grown at different substrate bias voltages.

Significant residual stress has been observed in cubic BN films of this thickness (> 500 nm).[18] UMich sample 051907 is pictured in Figure 18 (substrate length is 3.8 cm). The contours of the interference fringes (with the larger stress gradient in the long direction, and a smaller stress gradient in the transverse direction) indicate that the strain is mainly longitudinal. This assertion is confirmed by noticeable bending of the Si (100) substrate such that the sample has a slightly convex bowing (in the upwards direction of the picture), with the larger component of curvature in the longitudinal direction. The growth conditions for this sample were: substrate temperature = 1000°C, substrate bias = -120 V, pressure = 3 mTorr, N_2 flow = 5 sccm, Ar flow = 5 sccm, and RF power = 250 W. The reduced bias film growth technique is expected to significantly reduce the residual stress in thick films.[17]
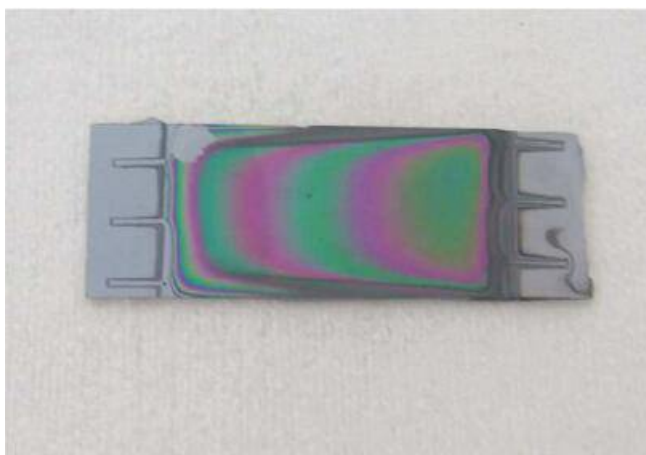

Figure 18. Cubic BN film sample (UMich 051907).

BN Film Structure

The micrographs of Figure 19, obtained using an atomic force microscope (AFM), show the surface morphologies of cBN films grown under identical conditions at three different thicknesses (50, 80, and 430 nm). Each scan covers an area of 1 μm × 1 μm. The comparison clearly shows the three stages of growth that cBN exhibits: nucleation, coalescence, and coarsening. The surface of the thinnest film (50 nm) shows nucleation of small islands with lateral dimensions of typically 20 to 50 nm. At a thickness of 80 nm, the nucleated cBN has coalesced to form larger islands 100 to 200 nm across, and at a larger thickness (430 nm), some coarsening is evident, accompanied by an increase in surface roughness. The root mean square (RMS) surface roughness was approximately 8 nm at nucleation, falling to 2 nm at coalescence, and rising to 9 nm in the thickest film.

The high resolution SEM micrograph of Figure 20 (with view normal to the substrate plane, looking at the film top surface) confirms the coarsened compact grain structure resulting from this sequence of growth steps after a total thickness of approximately 500 nm. The cBN film grows in a columnar mode with the grains extending from the substrate to the surface. This columnar geometry is favorable for detector applications in which the charge is transported by a potential gradient normal to the film (scattering from grain boundaries is minimized).
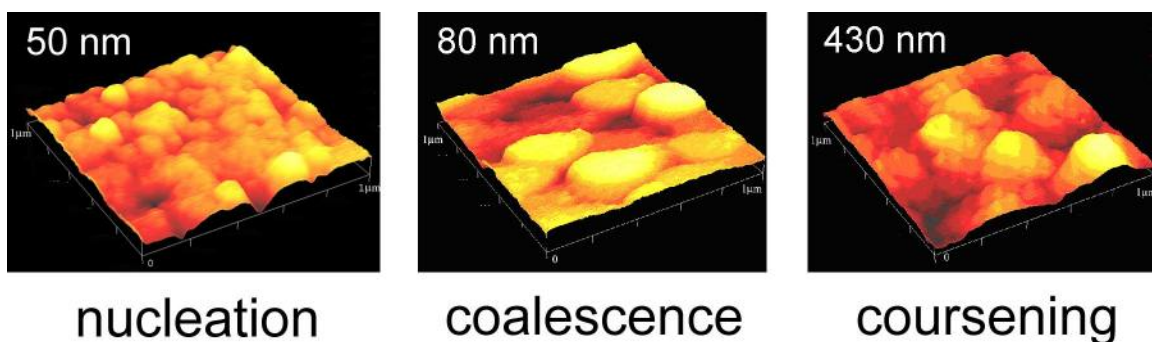
Figure 19. Three stages of cBN film growth.
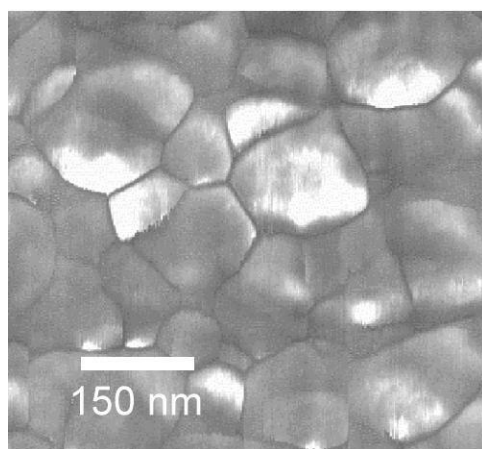
Figure 20. Grain structure of a 500-nm-thick cBN film.

The transmission mode FTIR spectrum was used to help identify the phase composition of the BN film. TO phonon peaks were observed at 1384 cm^{-1} and 767 cm^{-1}, indicative of the hexagonal phase. For these measurements, the Pt coating on the Si substrate backside (see the BN FILM GROWTH AND CHARACTERIZATION section) was removed.

Figure 21 shows a cross-sectional SEM image of UMich cBN film sample 021307 taken with an FEI Nova™ SEM acceleration voltage of 10 keV. The image was taken parallel to the Si substrate plane. The scale bar indicates that the film is approximately 100 nm thick, consistent with the purple interference color of this sample. Note that the thickness is very uniform and there are no pinholes in the film within the field of view. Note also that the SEM image of the BN film columnar microstructure confirms that the first 30 nm or so next to the Si substrate are dominated by hBN crystallites with the basal planes perpendicular to the substrate. The morphology depicted in the figure is very favorable for detector applications in terms of the columnar structure, uniformity of the film thickness, smoothness of the interface, and the absence of pinholes in the film.

Figure 21. High-resolution cross-section SEM image of a cBN film.

CARRIER LIFETIME MEASUREMENT RESULTS

Ultra-Fast Photon Correlation Fluorescence Measurements

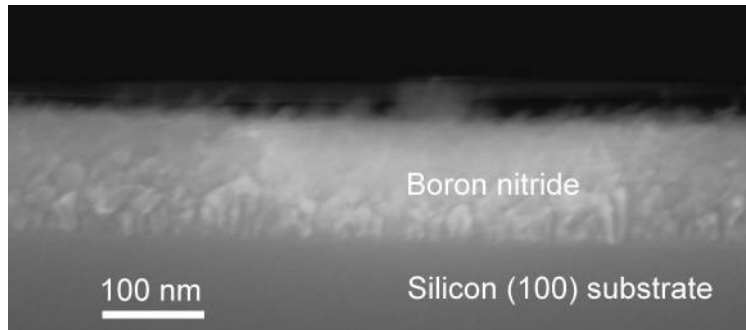Results of BN carrier lifetime measurements using an ultra-fast photon correlation fluorescence (PCF) technique (see the CARRIER LIFETIME MEASUREMENT METHODS section) are shown in Figure 22. All measurements were made at ambient temperature. Typical decay curves are shown for a plain Si wafer (coated with native oxide but without a BN film) and for a BN film deposited on Si. The fluorescence was routed, via a single-mode fiber, to a spectrometer so that fluorescence at different photon wavelengths could be measured. The data in the figure were measured at 550 nm (bare Si) and 560 nm (cBN on Si), corresponding to carrier excitation above the indirect band gap of silicon (about 1100 nm). Note that the fluorescence photon energy in this case is also greater that that of the laser fundamental. Thus, the excitation mechanism must involve non-linear processes such as two-photon excitation and second harmonic generation (400 nm). These measurements demonstrate that copious fluorescence occurs in a BN film on Si, even at 430 nm. The spectrometer–detector combination used was not optimized below this wavelength, making it impossible to probe deeper-lying trap states.

Note the two time scales in the decay curve of Figure 22. A strong, prompt signal exists between t = 0 and about 1 ns, followed by a much weaker signal that decays with a longer decay time of about 2.4 ns. The prompt signal likely resulted from luminescence centers near the surface of the wafer. The weak, slower decay signal was probably spurious. The carrier lifetime was extracted from these curves by extrapolation of the prompt signal decay.

The sensitivity of this measurement to surface states is enhanced because the excitation energy is well above the absorption gap for Si, and so the wafer is highly absorbing. Recombination is there-fore dominated by states in near the surface (within a few tens of nanometers). Interestingly, when the same measurement is performed on a thin film (about 60 nm thick) of cBN deposited on a Si wafer, the prompt decay peak broadens but the long decay is practically unchanged.

Compared to the bare Si data (Figure 23), the fast decay of luminescence (giving the carrier life-time) in cBN on Si is significantly longer, depending on the fluorescence wavelength probed. The solid lines in the figure are guides to the eye. The ~ 300 ps decay time at 560 nm is consistent with measurements obtained previously[2] using pump-probe optical reflectivity techniques at a somewhat longer probe wavelength (800 nm). The longer delay times seen in the figure could not be measured by the single-laser pump-probe method because of mechanical delay rail limitations (a maximum

delay time of about 500 ps). The nanosecond time scale of the lifetime measurements presented here confirms the need for the dual fiber laser system described in the CARRIER LIFETIME MEASUREMENT METHODS section. Delay times of up to 10 ns are specified for that system.
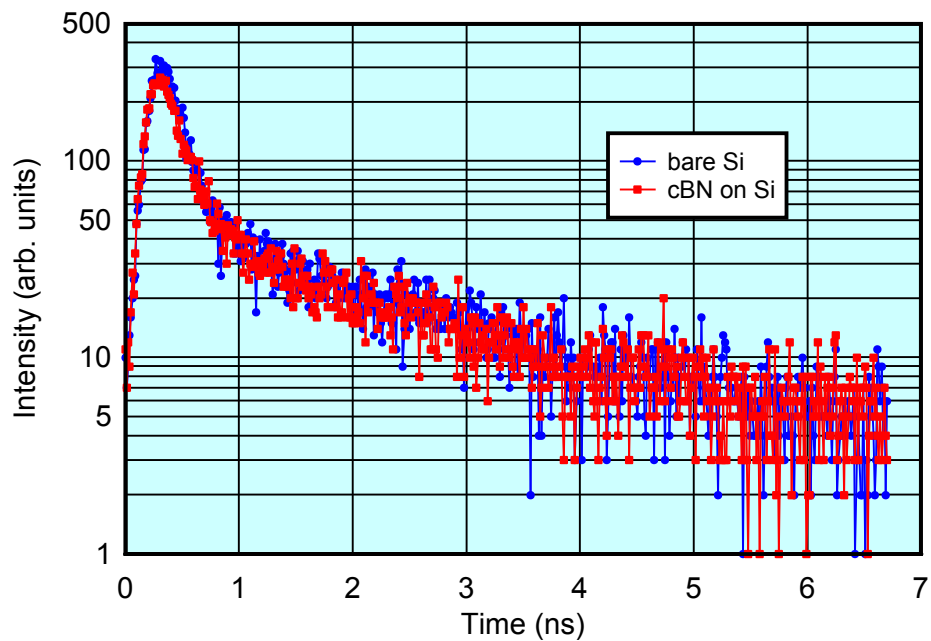

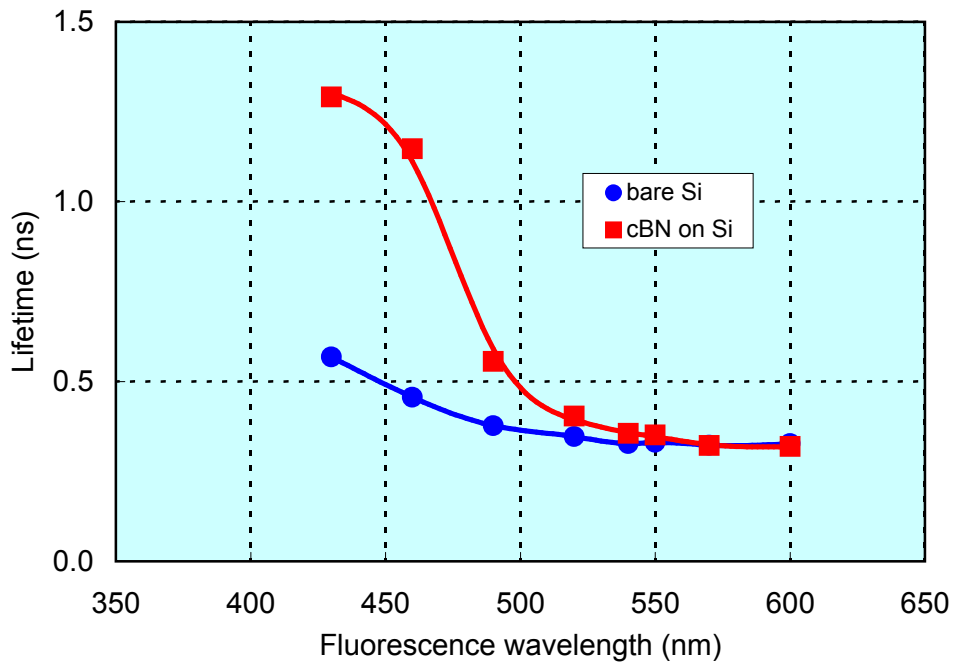Figure 22. Fluorescence data for bare Si and a cBN film on Si.

Figure 23. Carrier lifetime versus wavelength for cBN on Si compared to bare Si.

The BN layer seems to have the effect of passivating surface states or fluorescence centers that may be associated with the Si native oxide layer (on the bare Si sample of Figure 23). BN grown on Si under UHV conditions has no such oxide layer. The increased time constant of the decay of the charge carriers at the BN-Si interface is encouraging because long charge carrier lifetimes are required for detector operation. Note that the BN is expected to be transparent to the excitation laser frequency, at least up to third harmonic and possibly fourth harmonic (200 nm) wavelengths. Therefore, the bulk of the charge carriers are undoubtedly generated at the BN-Si interface during this measurement.

The fluorescence lifetime for the bare Si wafer increases slightly as the wavelength decreases. On the other hand, for BN films on Si, the prompt lifetime increases substantially as the wavelength decreases. This behavior suggests that the more energetic carriers have substantially longer lifetimes than those carriers that are excited to states just above the BN band gap.

The BN-Si interface region plays an important role in determining the lifetime of charge carrier transport for radiation detection applications. The charge carrier lifetime is expected to depend strongly on the density of electronic states in the detector material. Since the detected charge is produced close to the interface between the BN and the Si substrate, it is important to characterize the electronic density of states in this region. For this purpose, diffuse optical reflectivity measurements close to the Si band edge absorption were made on thick (500 nm) cBN on Si (100) samples. These measurements were done to determine the influence of the cBN film on the electronic density of states of the Si subrate near the film-substrate interface. The Si band gap is in the near infra-red (NIR) region of the electromagnetic spectrum, at a wavelength of approximately 1100 nm.

The sample was probed in reflection geometry with white light from a tungsten halogen lamp, and the spectrum of the diffusely reflected light measured. The spectrum, shown in Figure 24, exhibits a prominent absorption edge at the wavelength corresponding to the smallest band gap of the combined substrate (Si) and film (cBN) system. Photons with energies above this band gap are strongly absorbed, whereas photons at smaller energies (longer wavelengths) are reflected, hence the rapid increase in reflected intensity for wavelengths above about 1100 nm in the diffuse reflectance spectrum.

Since the Si band gap is ~ 1.1 eV and that of cBN is much larger (> 6 eV), the substrate band gap dominates the spectrum in the NIR. To measure the NIR spectrum, a spectrometer sensitive to this range of electromagnetic radiation must be used. A Control Development model NIR-256-1.7T1 indium gallium arsenide (InGaAs) array spectrometer was used for this purpose. This instrument can measure spectra in the 900 to 1700 nm range.

The results shown in Figure 24 are a comparison of the absorption edge of the silicon substrate before and after the cBN film is deposited. In both cases, a very sharp, well-defined edge is observed, indicating that the interface density of states is not strongly perturbed by the presence of the cBN film. There is, however, a systematic shift of the edge by about 14 nm after the cBN film is deposited on the silicon wafer. This corresponds to a shift in energy of about 15 meV, which is comparable to what is observed in lightly doped silicon. The shift of the band-edge is likely caused by free-carrier absorption at the interface between the silicon and the cBN, and reflects the density of states introduced by the cBN film. The states that are involved in this mechanism are relatively shallow (15 meV) and are not likely to affect the more energetic charge carriers expected to dominate the operation of the neutron detector. Note that these more energetic charge carriers (2 eV and greater)

showed the longest lifetimes (on order of nanoseconds) in the photoluminescence measurement results of Figure 23.
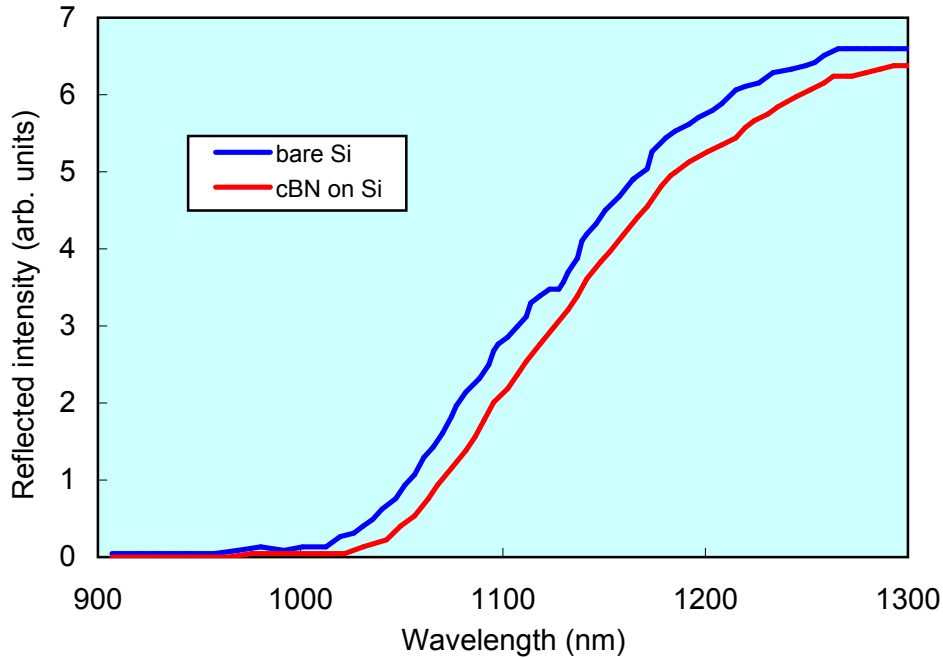

Figure 24. Reflectance versus wavelength for cBN on Si compared to bare Si.

These results indicate that the density of states resides close to the Si band edge. This optical reflectivity probe is sensitive to electronic states at the interface between the Si substrate and the BN film because the BN film is transparent to IR, whereas Si is strongly absorbing just above the band edge. The probe is therefore sensitive to electronic states in the Si immediately under the film. The reflectivity shift is relatively small (~ 15 meV) when the BN film is deposited, so the states introduced by the film must be close to the Si band edge. By comparison, the Si band gap is ~ 1.1 eV.

Also note that the sharpness of the absorption edge is preserved when the BN film is deposited on a Si substrate, indicating few structural defects in the BN. Additionally, the interface states are relatively shallow (< kT at temperature T = 300K, where k is Boltzmann's constant), so they will not be very effective as trapping centers for charge carriers. Therefore, the interface states are not a significant concern for the operation of a neutron detector, which requires nanosecond lifetimes at this film thickness (a few microns) for reasonable values of carrier mobility. Carrier lifetimes on this time scale were confirmed by the time-resolved fluorescence measurements. For carrier trapping, the depth of the trapping states is more important than the density of states. Similar concerns apply to Si metal-oxide-semiconductor (MOS) devices and to gallium arsenide (GaAs) high-electron-mobility transistor (HEMT) devices, but these applications are much more demanding with respect to charge carrier mobility.

Time-Resolved Reflectivity Measurements

Upon delivery of the Menlo Systems dual fiber laser system in mid-January 2007, various tests were performed to check compliance with specifications. As seen in the optical cross-correlation data of Figure 25, full-width half-maximum (FWHM) pulse widths of 88 and 155 fs were obtained

for the slave and master lasers, respectively, at an output wavelength of 1550 nm and average power of approximately 150 mW.

For some of its mode-locked states, the pulse width of the master laser was greater than the specified 150 fs. However, a mode locked state that was within specification could be selected by manually adjusting the polarizers on the master laser. The slave laser performs as specified (maximum pulse width of 150 fs) for all automatically selected phase-locked states; it is very stable and does not require manual adjustment. With manual adjustment, pulse widths of less than 80 fs were achieved for both lasers.

Taking advantage of the system's two-color capability, the frequency of one of the output beams was doubled (wavelength of 1560 nm halved to 780 nm). The 780-nm beam (at an average power of ~ 50 mW) was then used as the pump beam, and the 1560-nm beam as the probe beam.
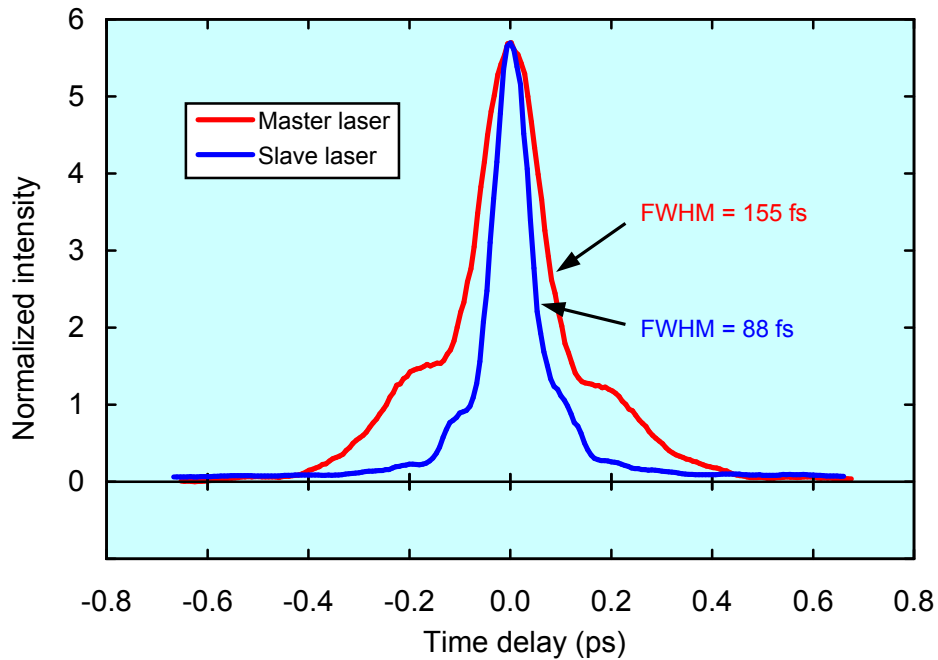

Figure 25. Pulse width measurement for master and slave fiber lasers.

For comparison with the known behavior of a standard direct-gap semiconductor, the carrier lifetime curve of Figure 26 (oscilloscope screen shot) was obtained on an AlGaAs–GaAs superlattice sample in which the AlGaAs band gap is smaller than the frequency-doubled photon energy and therefore strongly absorbing for the 780-nm pump beam. The two peaks are separated by the repetition interval of the laser oscillation frequency (100 MHz), giving a maximum time delay of 10 ns. The carrier lifetime in this case was 1.6 ns, consistent with accepted values for this type of III-V sample.[19] The data points were averaged over 512 traces of a digital sampling oscilloscope.

Two-color operation of the dual laser system enables separation of the TRR signal from the diffuse background for samples with significant surface roughness. This capability was used for bulk pBN sample BLK22. Previous measurement attempts using the single-laser pump-probe system of

Figure 4 were unsuccessful for this sample. With the two-color capability of the dual laser system, a weak time-resolved signal was measurable for this sample (see Figure 27). The relaxation lifetime was very short (~ 40 ps), however, so the pyrolytic form of BN is unlikely to be useful for neutron detector applications. Note that the time base in Figure 27 is greatly expanded relative to that of Figure 26, indicative of the much slower carrier relaxation in the pBN sample.
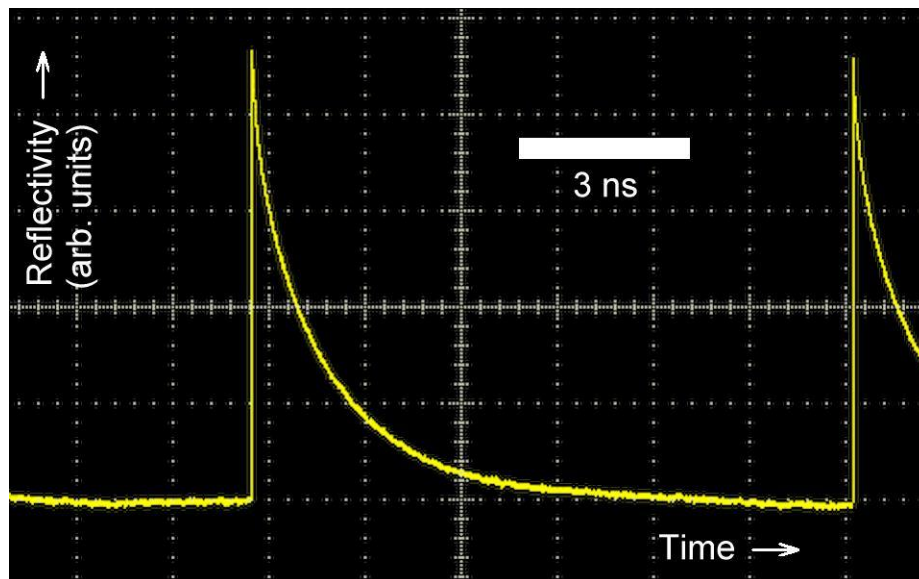

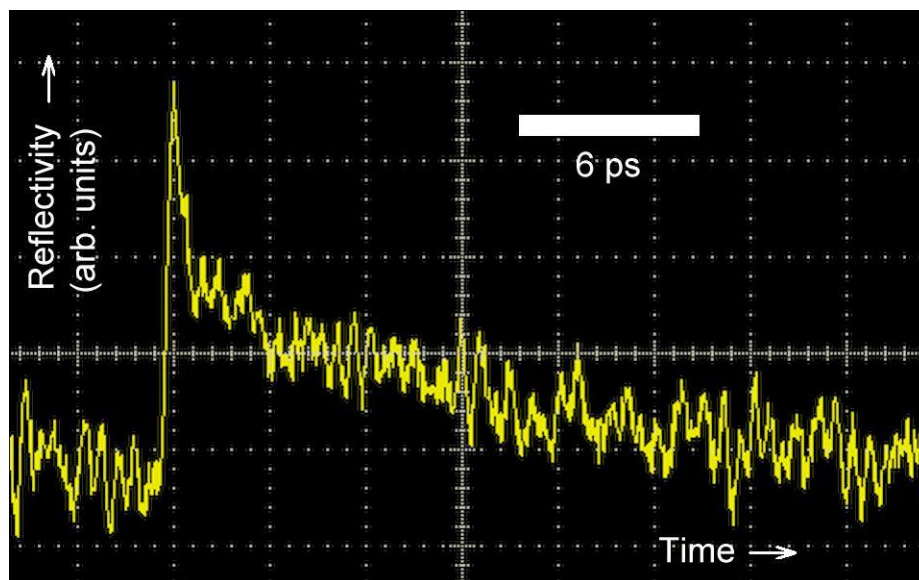Figure 26. TRR data for AlGaAs–GaAs superlattice sample.

Figure 27. TRR data for a bulk pyrolytic boron nitride (pBN) sample.

Similarly, UMich hBN film sample 031507 (480 nm thick), grown under non-stoichiometric conditions, has a measured carrier lifetime of 50 ps (see Figure 28). By contrast, hBN film sample

OUT111 (grown for approximately 10 hours to a thickness of ~ 250 nm) has a very smooth surface and showed a relatively long carrier lifetime (~ 3 ns); see Figure 29. The small ripples in the middle of the trace were caused by laser instabilities. As seen in Figure 2, a BN detector element with this carrier lifetime and a sample resistivity of 4×10^8 Ω-cm would require a carrier mobility of at least 7×10^4 cm^2/V/s.
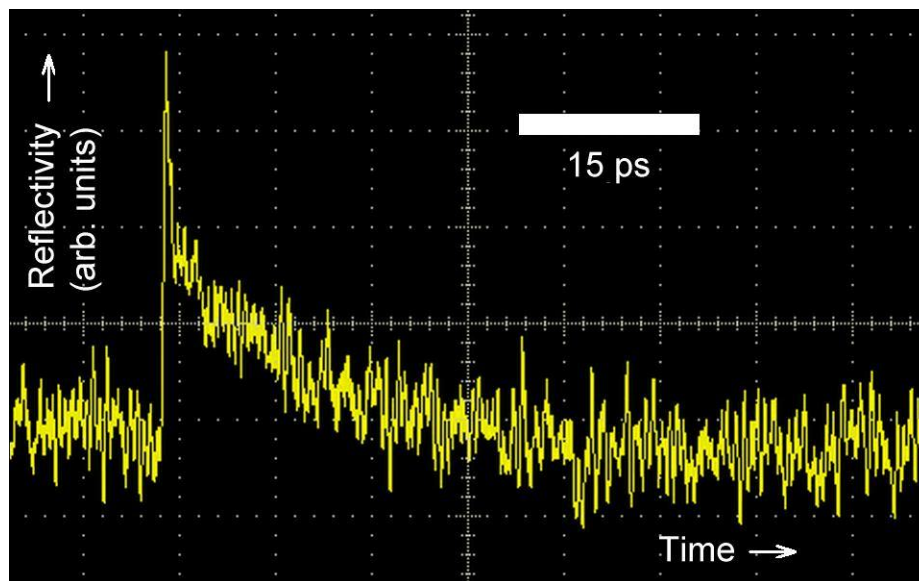

Figure 28. TRR data for 480-nm-thick hBN film grown on Si (100).
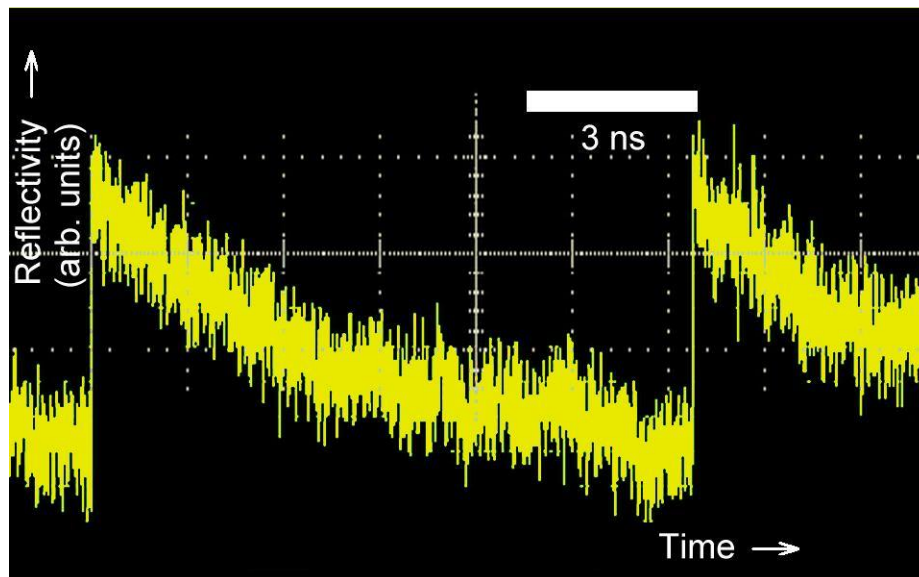

Figure 29. TRR data for 250-nm-thick hBN film grown on Si (100).

CARRIER MOBILITY MEASUREMENT RESULTS

For the corona triode measurements of BN carrier mobility, the sample surface voltage is equal to the difference between the applied grid voltage and the grid-to-sample-surface (air gap) voltage drop. For constant sample and corona currents (I_{corona}), the air gap voltage is a constant. The air gap voltage is determined by measuring the current flowing to the sample holder (which is at ground potential) when there is no sample in place (with the same air gap distance between the grid and the sample holder as there would be if a sample were mounted on the holder). An example of this so-called "no sample" current measured as a function of grid voltage (using, for this purpose, constant voltage high-voltage corona and grid power supplies) for various corona-point-to-grid distances and corona currents is shown in Figure 30 and Figure 31.

Hexagonal BN film sample OUT111, attached to a copper-clad printed circuit board as in Figure 10, was mounted in the corona triode apparatus of Figure 8. The backside contact was connected to circuit ground through a Keithley® 6517 electrometer. The wire connected to the top gold electrode had been carefully removed. Although a top electrode is not needed for measuring carrier mobility with this apparatus, it should have no deleterious effect on the measurement, assuming it is in contact only with the top surface of the BN film. The charge deposited on the sample surface perhaps covers the surface more uniformly than it would without the electrode, but that should have no effect on the results.

Because sample OUT111 is very thin (250 nm), the transit time given by Equation (11) will be on the order of a few milliseconds or less, even for low currents (nanoamps), large sample capacitance (nanofarads), and low carrier mobility (10^{-3} cm^2/V/s or higher). Steady-state conditions will therefore be reached very quickly, and so the mobility is most easily determined using Equation (10).
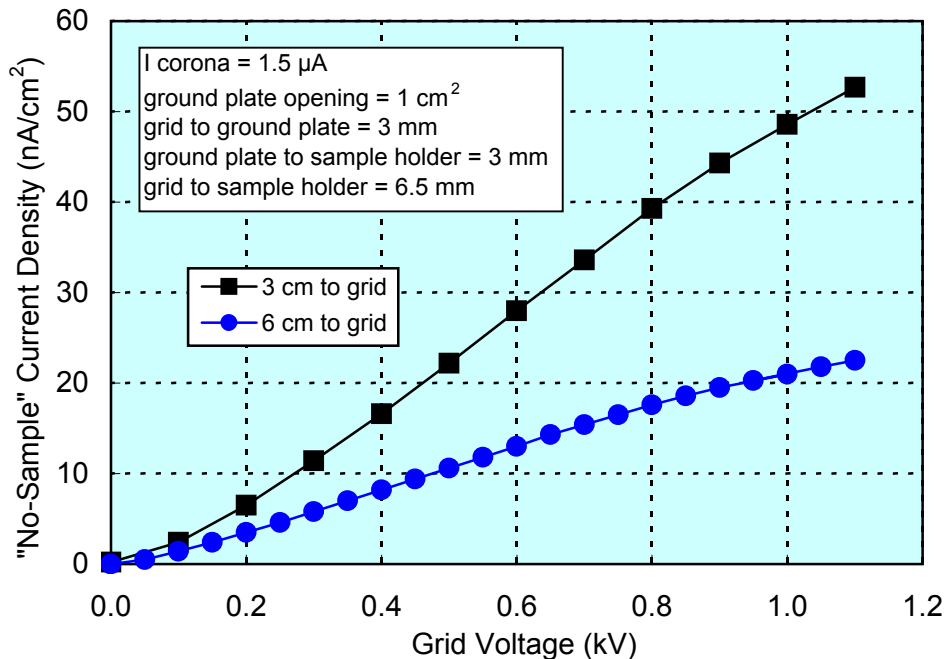

Figure 30. "No-sample" current density data for two corona-point-to-grid distances.
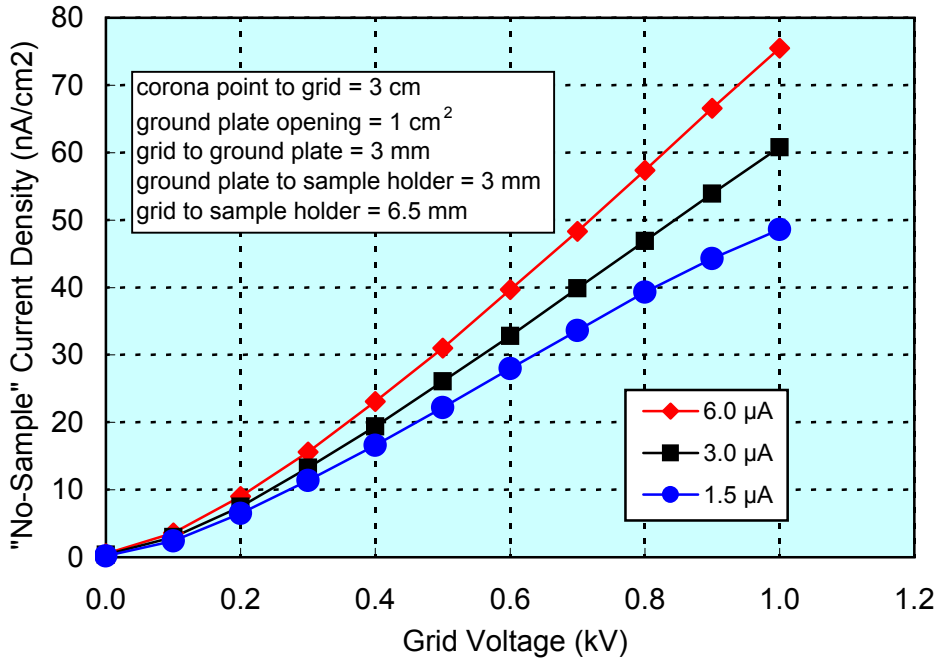
Figure 31. "No-sample" current density data for various corona current densities.

The sample current of hBN film OUT111 was measured as a function of sample surface voltage using the corona triode apparatus under the following conditions:

- Grid material: 80 mesh stainless steel
- Corona-point-to-grid distance: 10 mm
- Grid-to-sample-surface distance: 1 mm
- Corona current: 4 μA (maintained constant within ± 1%)
- Sample area exposed to corona discharge: 26.6 mm^2
- Time between data points: 30 s
- Each current value averaged over 75 readings.

A thin plastic spacer (0.5 mm thick) was used to electrically isolate the top sample surface from the ground plate of Figure 8. The resulting I-V data are shown in Figure 32 on a log-log scale.

Figure 32. Current–voltage data for hBN film measured with the corona triode.

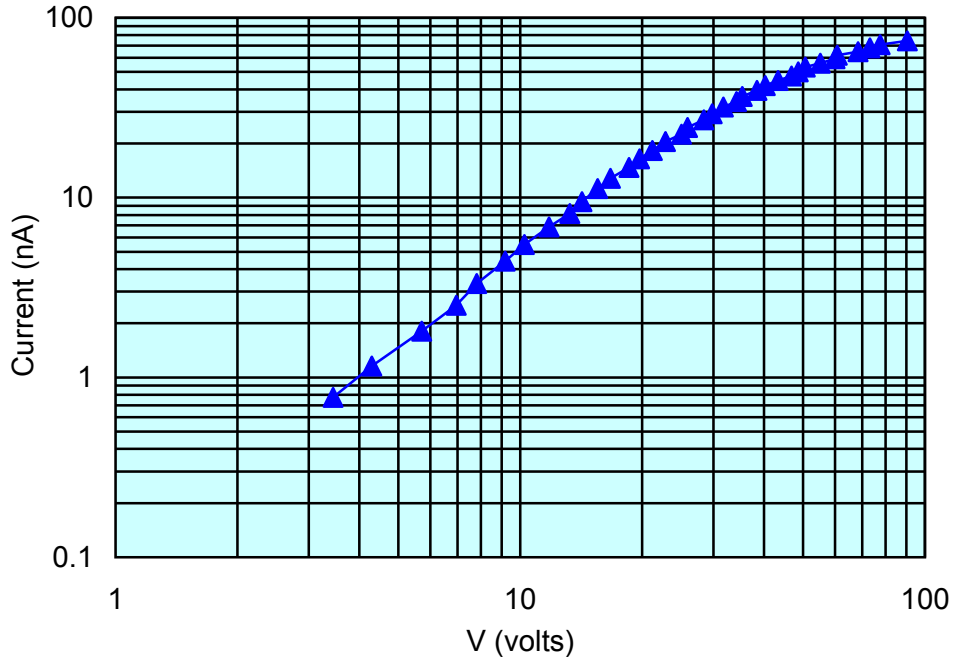For the low-voltage portion of Figure 32 (up to ~ 10 V, corresponding to an electric field of 4×10^5 V/cm), the current increases in proportion to V^2, as expected from Equation (9). At higher voltages, the current increases more slowly with voltage, presumably because of high-electric-field effects.[10] Using the low-voltage data with Equation (10), the effective (trap-modulated) mobility of this sample is estimated to be ~ 6×10^{-12} cm^2/V/s. From Equation (11), however, the expected time to reach a steady-state current value is about 15 to 30 s, much longer than actually observed. This inconsistency casts doubt on the obtained mobility value. Further measurements will be required to resolve this uncertainty. Previously, Hall effect measurements on semiconducting cBN films gave Hall mobilities of 200 cm^2/V/s (reference 20) to 500 cm^2/V/s (reference).

ELECTRICAL PROPERTIES

Electrodes

The BN films are currently grown on Si substrates, which can serve as the backside electrode for a FIND device if the BN-Si contact resistance is low enough (i.e., small compared to the resistance through the BN thickness). A low-resistance, ohmic contact to the free surface of the Si is therefore most desirable. One way to form this contact is by depositing an aluminum (Al) film on the Si and then annealing the contact at about 450 to 480°C in an inert atmosphere. To ensure that this contact method works, *in situ* resistance versus temperature and current versus voltage measurements were made between two aluminum contact pads that had previously been deposited onto the polished surface of a Si wafer and photolithographically patterned. The results obtained during furnace heating in flowing Ar are shown in Figure 33 and Figure 34. In Figure 34, the voltage values are normalized to those at I = 1 mA to show the transformation from non-linear to ohmic behavior.
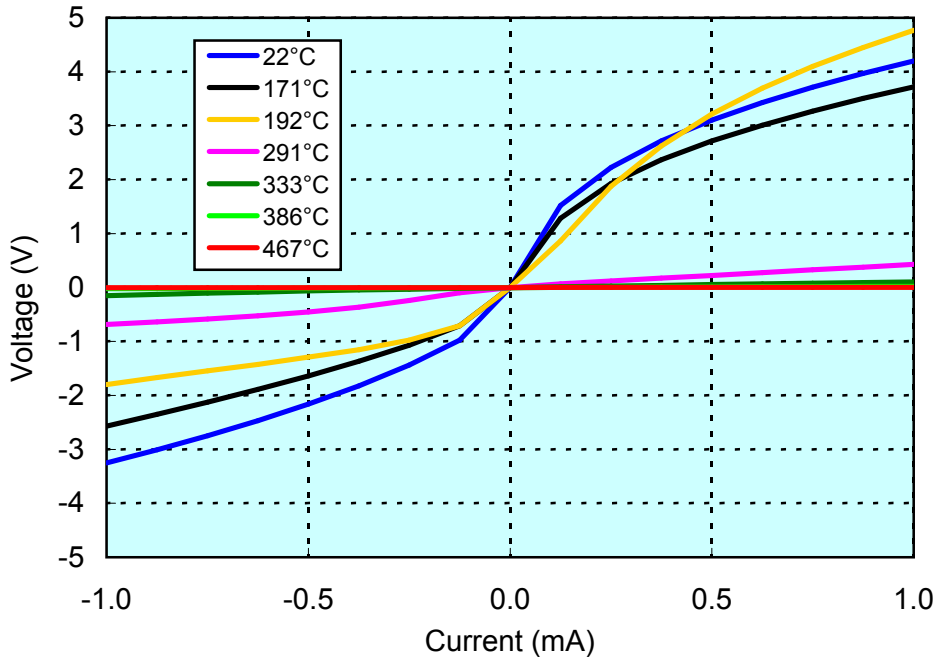
Figure 33. Current–voltage data measured between two Al contacts on Si.
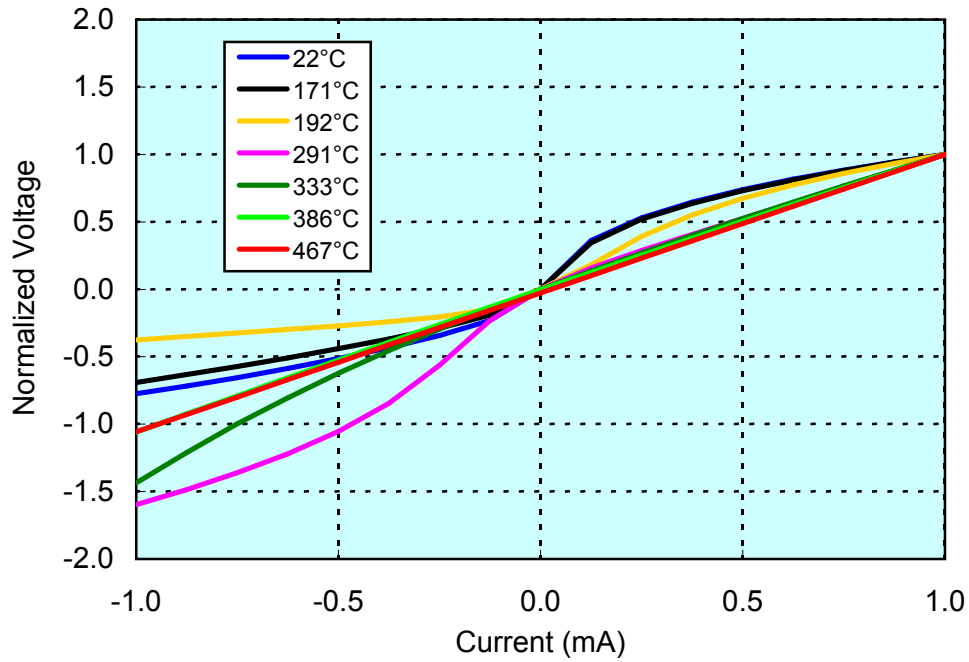

Figure 34. Al contact data of Figure 33 with normalized voltage scale.

The ohmic behavior is maintained after cooling to room temperature. The resistance between the two Al contacts (measured at $I = 10^{-5}$ A) during furnace heating and cooling is shown in Figure 35.
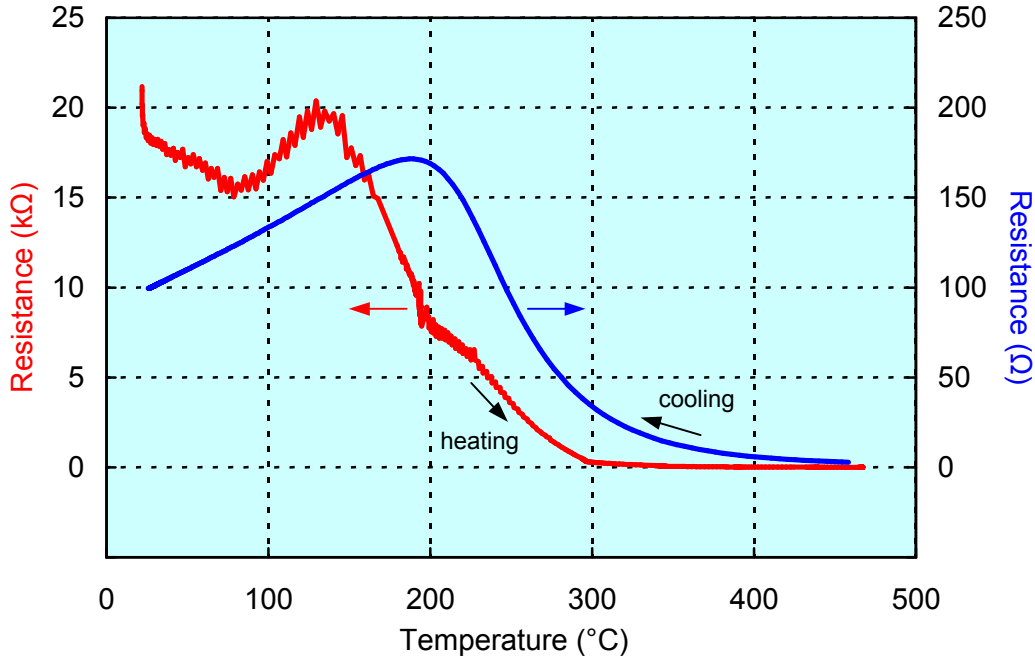
Figure 35. Resistance between two Al contacts on Si during furnace annealing.

To ensure that an ohmic contact could be made to the backside of the actual wafers used as substrates for the BN films, and that a silver contacting layer on the aluminum would not degrade the contact, a pair of Ag/Al contacts were ion beam sputter deposited on the Si backside of BN film sample OUT108. The sample was annealed for 30 min at 480°C in flowing Ar gas, and I-V measurements made during sample heating and cooling. After cooling to room temperature, the I-V curves were linear. The room-temperature resistance between the two contacts was reduced from 133 Ω (before annealing) to 63 Ω (after annealing).

Because of the extremely high resistivity of BN, measuring the contact resistance of electrodes on BN is very difficult. First, the current that flows between two contacts is very small because of the high BN resistance, and second, the contact and BN contributions to the resistance cannot be separated. The measurement is complicated even further for BN films on a relatively conducting substrate, such as Si.

In an attempt to overcome the first obstacle, multi-layer Ag/W/Ti films (film sample FLM178) were deposited on the surface of a sheet of free-standing pBN (sample BLK24). The metal films were lithographically patterned and wet-etched[2] to form two closely-spaced interdigitized electrodes (see Figure 36). Silver wires were connected to the electrode pads using silver paint.

Figure 36. Interdigitized electrodes on pBN sample.

The current flowing between these electrodes was measured with an electrometer as a function of applied voltage (up to 500 V) between the electrodes (before any annealing; see 22°C curve of Figure 37). A series of annealing steps under flowing Ar was then performed to react the Ti layer with the BN, and thereby reduce the contact resistance. The sample was heated to ever increasing temperatures (for 1 hour at anneal temperatures between 510 and 900°C). The current–voltage curves were again measured after each annealing step once the sample had cooled to room temperature (see Figure 37).
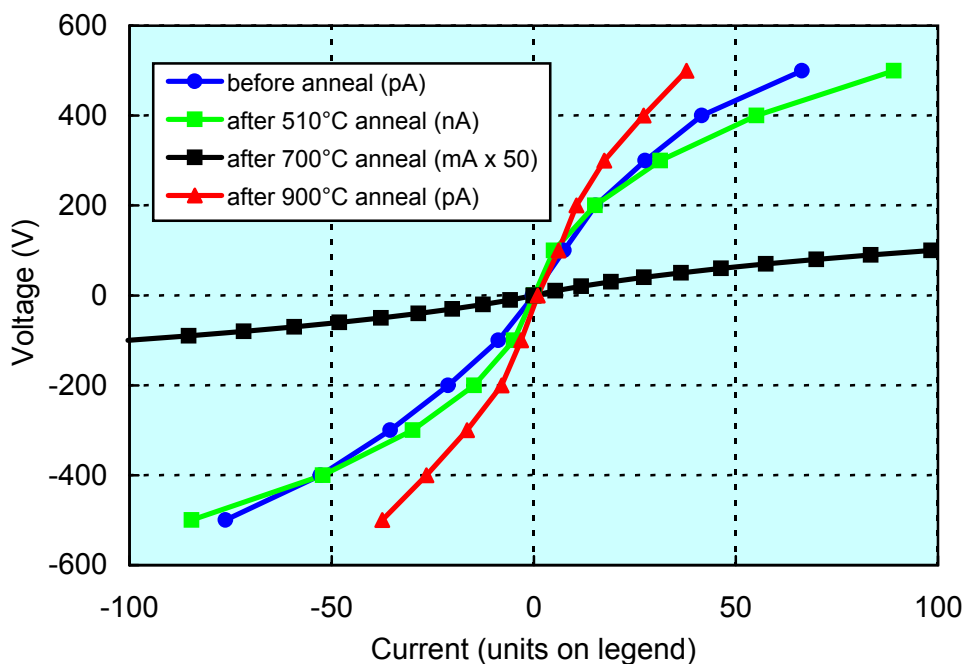
Figure 37. Current–voltage data for pBN sample of Figure 36 before/after annealing.

Note the different units for current for the various curves in the figure; the maximum current for the sample annealed at 700°C is about 2 mA. From these measurements, the total resistance measured between the contacts dropped dramatically as the sample was heated to temperatures reaching 700°C. This low resistance value may be caused, however, by sublimation of the silver paint, wires,

and/or top electrode film, and subsequent silver condensation onto the sample surface upon cooling (partially shorting out the electrodes). After the 900°C anneal, the resistance was higher than the initial value (before any annealing). This higher value indicates that any condensed silver coating evaporated away, and that perhaps the contact at the Ti-BN interface had become degraded (possibly because all of the Ti had reacted, after which the W might start to react with the Ti-BN reaction products, adversely affecting the contact resistance).

BN Films

The resistivity of various hBN film samples, about 250 nm thick, were first estimated using a 5-mm^2 sputtered gold electrode on the surface of the film and a platinum contact on the back of the Si wafer. BN resistivities in the range of 10^{10} to 10^{11} Ω-cm were obtained from resistance values measured at low voltage.

One hBN film sample (OUT94, ~ 324 nm thick) with an aluminum contact deposited by ion beam sputtering onto the Si substrate backside was used to measure the current–voltage (I-V) characteristic between two multi-layer Ag/TiN/Ti contacts (see Figure 38; the solid line is a linear fit to the data). The measurement was made between a 1-mm-diameter Ag/TiN/Ti circular contact to the hBN film and a large Al contact on the back of the Si wafer. The contacts on the hBN film had previously been deposited and patterned as a pair of 1-mm-diameter dots.
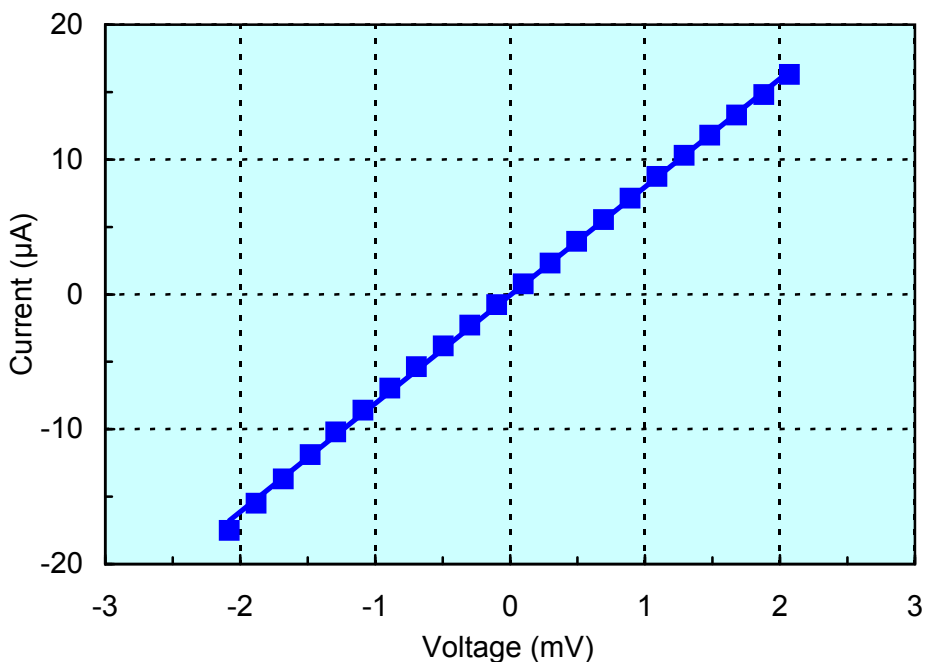
Figure 38. Current–voltage curve of hBN film (between front and back contacts).

To ensure that the measured current flows through the BN film (and not across the film surface), a silver paint (grounded) guard ring was formed around the sample edge and between the two dots. Before any furnace annealing of the sample, the I-V between the two dots, and between each dot and the Si backside, was measured. A similar guard ring and dot pattern was fashioned on a cBN film on Si sample (OUT106, ~ 243 nm thick) by patterning the Ag/TiN/Ti layer appropriately, and I-V

measurements were made. The I-V curves of both samples were essentially linear, indicating good ohmic contact between the metal electrodes and the BN films. However, the BN film resistance was much smaller than expected (perhaps because of pin holes in the thin BN films).

As described in the FIND Device Configuration section, hBN sample OUT111, with its promising carrier lifetime value, was configured as a FIND device with a sputtered 6-mm × 6-mm gold top electrode (see Figure 10). Ohmmeter measurements gave the following results:

- hBN film + Si substrate resistance: 42 kΩ with one polarity, 28 kΩ with the other
- Si substrate resistance: 2.7 kΩ
- hBN film resistivity: ~ 4×10^8 Ω-cm, measured at a voltage of 0.6 V.

THERMAL NEUTRON DETECTION RESULTS

The first device described in the FIND Device Configuration section was made with pBN sample BLK23 (with a BN thickness of 0.32 mm and a top electrode area of 0.55 cm^2). That device was tested by placing a small Am-Be neutron source (producing 10^5 n/s) within a few centimeters of the device (giving a neutron flux of about 500/cm^2/s). The source was surrounded by lead (to contain gamma rays) with an outer jacket of polyethylene (to thermalize the neutrons). A bias voltage of up to 600 V could be placed across the detector electrodes. At bias voltages up to 200 V, no pulses attributable to neutron bombardment could be seen (over times of about 1 min). This result indicates that the μτ product for this sample is less than about 2 to 3×10^{-6} cm^2/V. Higher bias voltages resulted in noise in the output of the charge pulse amplifier circuit that would have obscured any neutron-induced pulses.

The second device mentioned in the FIND Device Configuration section was based on hBN film sample OUT111. This device was also tested with the Am-Be neutron source as described above, but at much lower bias voltages. Because sample OUT111 is over a factor of 10^4 thinner than sample BLK23, a much lower bias voltage is needed to achieve the same electric field within the sample. From Equation (7), assuming a charge collection efficiency of 1 (no μτ limitations), the measured count rate for this 250-nm-thick sample (with $\sigma_m = 42.4$ cm^{-1} for hBN) is expected to be 11 to 12 counts/min.

For this hBN film sample, application of the bias voltage resulted in random noise at the charge pulse amplifier output. In the presence of the Am-Be source, and with applied bias voltages (V_{bias}) ranging from –2 to +3 V (applied across the series combination of the sample and two 1 MΩ resistors) , there was no clear indication that any counts were caused by neutron events. Any counts caused by such events would have been overshadowed by the numerous counts triggered by noise.

The noise, perhaps caused by the granular nature of the gold contacts or the BN film itself, increases with bias voltage (Figure 39) and would quickly obscure any current pulses generated by neutron events. This effect is seen in the figure as the test current pulse at t = 0 becomes more and more "hidden" by noise as the bias voltage is increased from 0 to 4 V. The test current pulse was generated using the attenuation circuit of Figure A-4. The temperature dependence of the noise is shown in Figure 40. The blue curves of Figure 40 were measured with $V_{bias} = 1$ V, while the red curve at 22°C was measured with zero bias voltage. The curves of Figure 39 and Figure 40 are offset vertically for clarity.
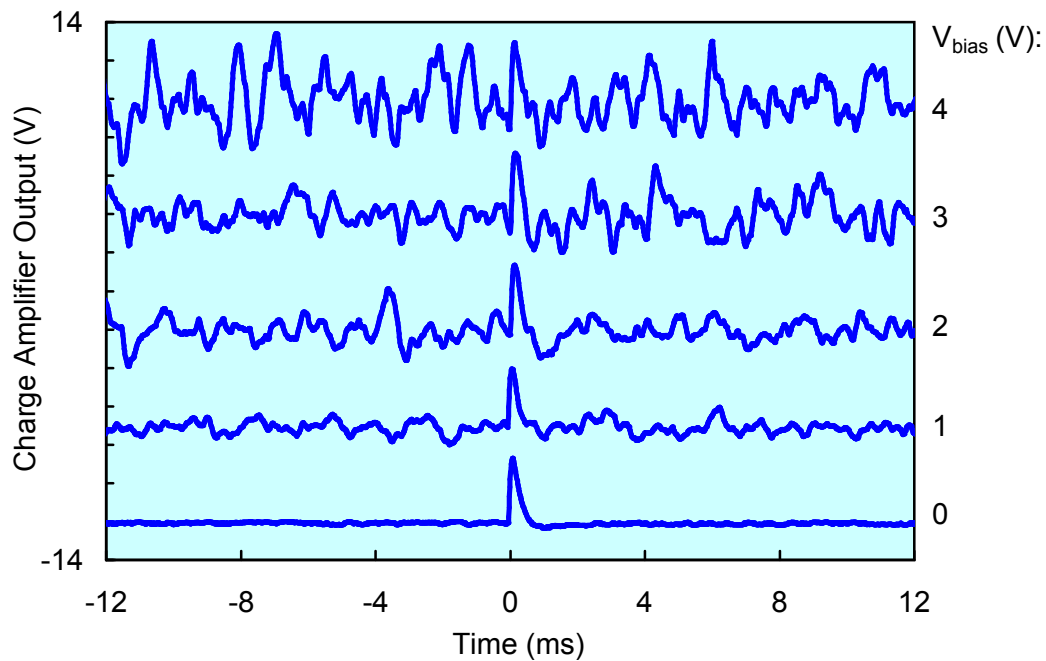
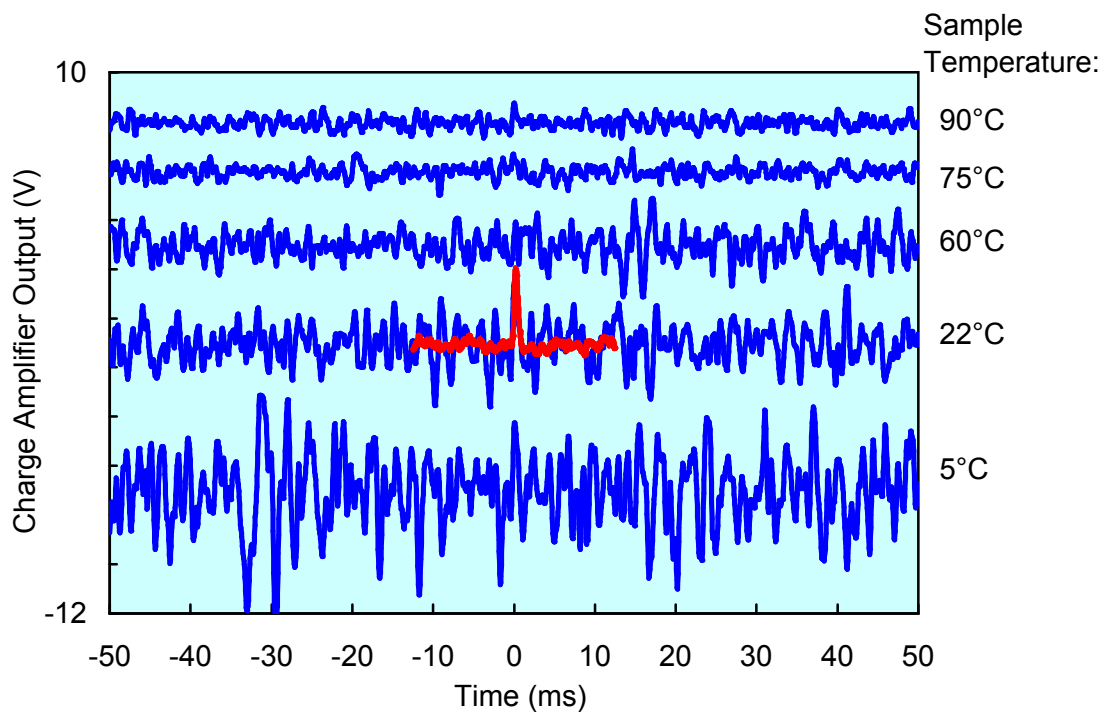Figure 39. Detector noise as a function of bias voltage for a 250-nm hBN film.

Figure 40. Temperature dependence of detector noise for the hBN film of Figure 39.

SUMMARY AND CONCLUSIONS

The techniques needed to measure the key boron nitride electrical properties of carrier lifetime and mobility were developed and implemented. Acceptable values of these properties, as well as reasonably good electrical contact to BN and sufficiently high BN resistivity, are needed for a working thermal neutron detector based on the FIND concept.

A new dual fiber laser system was set up at the UMich to measure the carrier lifetime of BN films and sheets using a time-resolved (or pump-probe) reflectivity method. The two-color capability of the new system enabled the characterization of bulk samples, which was impossible with a previously used single-laser system[2] because of noise produced by sample surface roughness. In addition, the phase delay between two lasers can be synchronized electronically, rather than mechanically as done previously.[2] The maximum measurable carrier lifetime therefore increased from 500 ps with the single-laser method to 10 ns with the dual laser arrangement.

A corona triode apparatus designed and built at SSC San Diego was used to determine the BN carrier mobility from the build-up or decay of a sample surface charge with time. Extraction of the mobility requires that the measurement be done under space-charge-limited, constant-current conditions. To ensure the latter condition, special feedback circuits for use with standard (constant-voltage) high-voltage power supplies were constructed.

Initial measurements of BN carrier lifetime and mobility were made using the methods and equipment described above. In parallel with this sample characterization effort, metal electrodes were deposited on a limited number of BN samples for evaluation as a neutron detector. The two samples (one a freestanding pyrolytic BN sheet, and the other a hexagonal BN film deposited on a silicon substrate) configured and tested as FIND devices gave a null detection result. A measured carrier lifetime value of 40 ps for the pyrolytic sample explains this result. The hexagonal film has a much higher carrier lifetime (3 ns), but initial measurements indicate a very poor mobility value for that sample, and thus free carriers generated by a neutron-boron reaction would not reach the detector electrodes. Based on previous measurements of semiconducting film samples, much higher mobilities are expected for cubic BN films. In addition, carrier lifetimes of several nanoseconds have been measured in cubic phase films.

A detector with directional capability is highly desirable. An SSC San Diego invention disclosure[16] has been submitted for a detector that can determine the incident direction of thermal neutrons. This omnidirectional detector would be formed from three orthogonal pairs of planar BN detector elements (FIND devices).

RECOMMENDATIONS FOR FURTHER DEVELOPMENT

Continuation of the work described above is needed to make a reproducible and reliable FIND device for detecting thermal neutrons. The newly applied sample characterization techniques, along with on-going improvements in BN film growth, can be used to test and optimize a solid-state detection element based on high-quality cubic boron nitride films. Based on the data reported here, of the various available forms of BN, cubic phase films seem to hold the most promise. Once individual FIND devices have been shown to work, and their properties optimized for the most efficient neutron detection, multiple FIND elements can be combined into a thermal neutron detector with directional capability.

REFERENCES

1. J. Losee, J. C. Hicks, E. W. Jacobs, W. C. McGinnis, and R. D. Boss. 2001. *Boron Nitride Solid State Detector for Thermal Neutrons*, U.S. Patent Disclosure, Navy Case No. 83098.

2. W. C. McGinnis. 2003. "Film Implementation of a Neutron Detector (FIND): Proof of Concept Device," SSC San Diego TR 1921 (Oct). SPAWAR Systems Center, San Diego, CA.

3. W. Shockley. 1938. "Currents to Conductors Induced by a Moving Point Charge," *Journal of Applied Physics*, vol. 9, no. 10, pp. 634-635.

4 . S. Ramo. 1939. "Currents Induced by Electron Motion," *Proceedings of the Institute of Radio Engineers*, vol. 27, no. 9, pp. 584-585.

5. K. Hecht. 1932. "Zum Mechanismus des lichtelektrischen Primärstromes in isolierenden Kristallen," *Zeitschrift für Physik*, vol. 77, pp. 235-245.

6. Y. Eisen, A. Shor, and I. Mardor. 1999. "CdTe and CdZnTe Gamma Ray Detectors for Medical and Industrial Imaging Systems," *Nuclear Instruments and Methods in Physics Research A*, vol. 428, no. 1, pp. 158-170.

7. D. Litvinov and R. Clarke. 1997. "Reduced Bias Growth of Phase-Pure Cubic Boron Nitride," *Applied Physics Letters*, vol. 71, no. 14, pp. 1969-1971.

8. S. M. Sze. 1981. *Physics of Semiconductor Devices*, 2nd ed., sec. 1.7.2, p. 52. John Wiley & Sons, New York.

9. D. J. Harris and P. N. Robson. 1974. *The Physical Basis of Electronics*, sec. 9.1.1, p. 168. Permagon Press, Oxford.

6. G. F. Leal Ferreira and M. T. Figueiredo. 1992. "Corona Charging of Electrets," *IEEE Transactions on Electrical Insulation*, vol. 27, no. 4, pp. 719-738.

11. J. A. Giacometti and J. S. Carvalho Campos. 1990. "Constant Current Corona Triode with Grid Voltage Control. Application to Polymer Foil Charging," *Review of Scientific Instruments*, vol. 61, no. 3, pp. 1143-1150.

12. M. A. Lampert and P. Mark,. 1970. *Current Injection in Solids*, ch. 4, p. 45. Academic Press, New York.

13. M. J. Russ. 1963. "Surface Conduction in Group II-VI Semi-Insulators," *Journal of Applied. Physics*, vol. 34, no. 6, pp. 1831-1832.

14. K. L. Moazed, J. R. Ziedler, and M. J. Taylor. 1990. "A Thermally Activated Solid State Reaction Process for Fabricating Ohmic Contacts to Semiconducting Diamond," *Journal of Applied Physics*, vol. 68, no. 5, 2246-2254.

15. K. Kobayashi. 2000. *Development of a Balloon-borne Hard X-ray Spectrometer for Solar Flare Observation*, ch. 2, pp. 28-34. M.S. thesis, University of Tokyo.

16. W. C. McGinnis. 2007. *Omni-Directional Solid-State Thermal Neutron Detector*, U.S. Patent Disclosure, Navy Case No. 98557.

17. D. Litvinov, C. A. Taylor II, and R. Clarke. 1997. "Semiconducting Cubic Boron Nitride," *Diamond and Related Materials*, vol. 7, no. 2, pp. 360-364.

18. D. Litvinov, R. Clarke, C. A. Taylor II, and D. Barlett. 1999. "Real-Time Strain Monitoring in Thin Film Growth: Cubic Boron Nitride on Si (100)," *Materials Science and Engineering B*, vol. 66, no. 1-3, pp. 79-82.

19. N. K. Dutta, R. L. Hartman, and W. T. Tsang. 1983. "Gain and Carrier Lifetime Measurements in AlGaAs Single Quantum Well Lasers," *IEEE Journal of Quantum Electronics*, vol. QE-19, no. 8, pp. 1243-1246.

20. W. C. McGinnis. 2001. "Electronic Properties of Cubic Boron Nitride," *ILIR'00: SSC San Diego In-House Laboratory Independent Research 2000 Annual Report*, SSC San Diego TD 3115 (May), pp. 94-96.

APPENDIX A
CHARGE PULSE AMPLIFIER

Improvements were made in a previously built charge pulse amplifier circuit[2] based on an Amptek® A250 charge pulse preamplifier. The modified circuit (Figure A-1 through Figure A-3) is used to detect the current pulses produced when thermal neutrons react with ^{10}B in the FIND device.
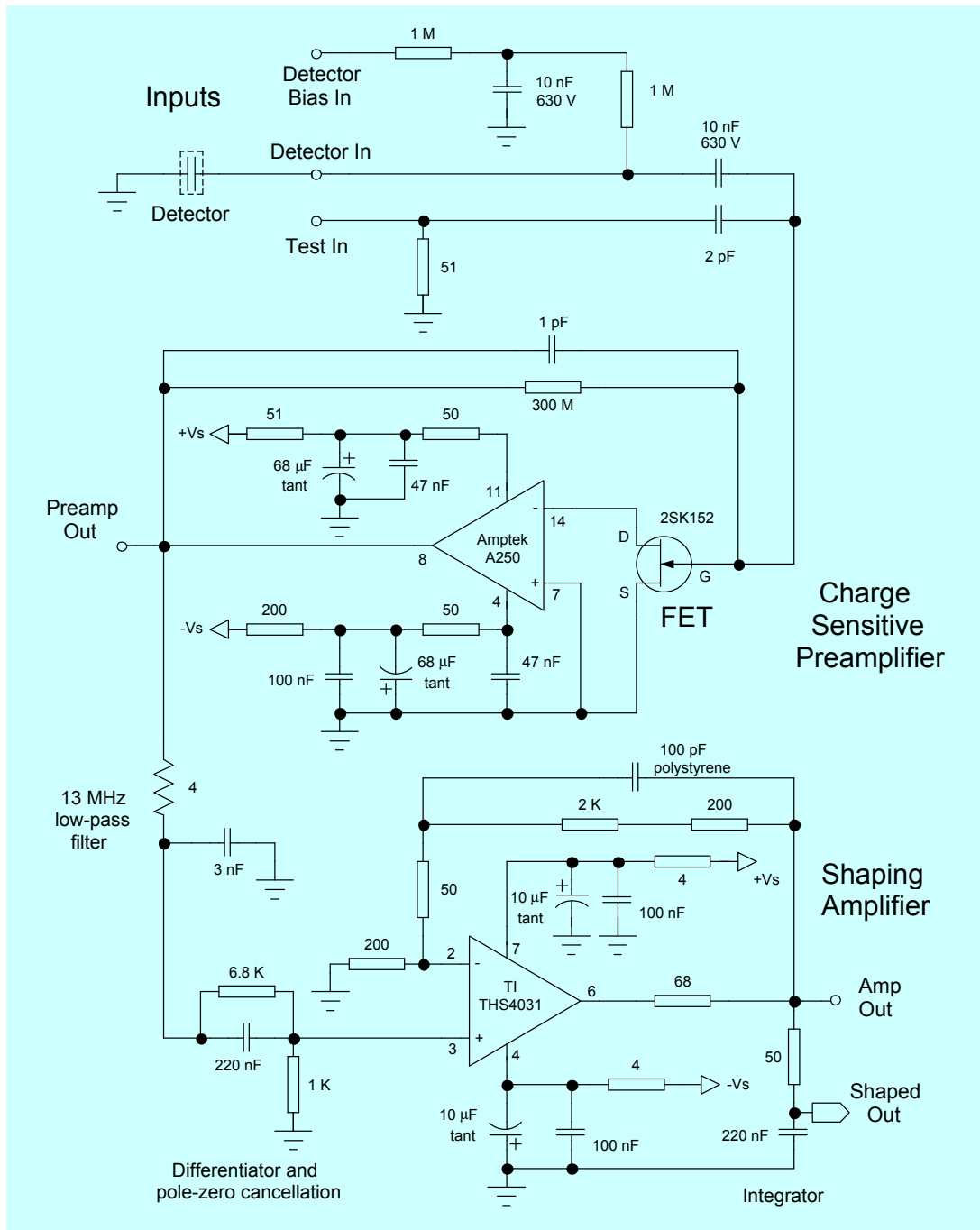

Figure A-1. Modified charge pulse amplifier circuit.

A few changes have been made in the charge pulse amplifier circuit compared to that shown in the previous FIND project report.[*] First, note the 1 MΩ bias resistor in the upper right of Figure A-1 (connected to the "Detector In" input). This value is required for a BN film detecting element in order to obtain the desired voltage drop across the BN (and therefore the desired electric field) without too high of a voltage drop across the bias resistor. For example, BN film sample OUT111 (250 nm thick) has a DC resistance of about 25 kΩ and a capacitance of 6 nF (at 10 kHz). For a thick bulk BN detecting element (with a thickness on the order of 100 μm, and therefore a much higher resistance than the film detecting element), a 100 MΩ resistor would be used instead. A direct consequence of using a thinner BN detecting element is that a much lower "Detector Bias In" signal level is needed compared to the thick detecting element (tens of volts rather than hundreds or thousands of volts).

Another change is that the Amptek® A250 output is taken from pin 8 (which includes a 100 Ω isolation resistor), rather than the previously used pin 9 (no isolation resistor). This change was made to reduce the capacitive load at the output, and helped eliminate output pulse ringing that was observed with a 10 kHz square wave test input.

The shaping amplifier time constants have also been adjusted for use with a BN film detecting element. The resistance-capacitance (RC) time constant τ_{RC} for sample OUT111, for example, is about 150 μs. This value must be considered when setting the differentiator and integrator time constants τ_D and τ_I, respectively. From Figure A-1, $\tau_D = (1 \text{ k}\Omega)(220 \text{ nF}) = 220$ μs and $\tau_I = (50 \text{ }\Omega)(220 \text{ nF}) = 11$ μs. Selecting $\tau_D \geq \tau_{RC}$ ensures that the detector collects all collectable charge. This value for τ_D, combined with a relatively small value for τ_I, maximizes the output pulse height while collecting all available charge. These choices also seem to give the best signal-to-noise ratio, although the count rate will be limited by pulse overlap.

A post-output amplifier (Figure A-2) was also added to increase the amplitude of the shaped output pulse from about 30 mV to a maximum of about 3 V (for a 16 mV input pulse to the 2 pF test capacitor). This modification ensures that any neutron-induced pulses can easily be seen by a pulse counter or an oscilloscope.
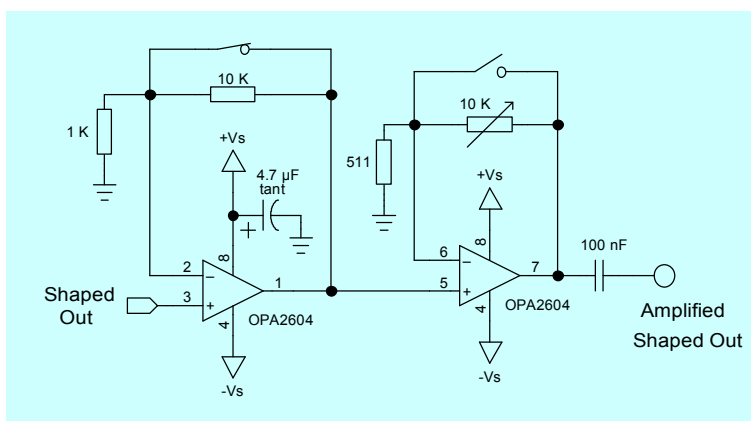

Figure A-2. Amplifier for shaped output of charge pulse amplifier shown in Figure A-1.

[*] Also note that corrections to the circuit schematics shown in the previous report[2] are listed in Appendix C. These corrections are included in the schematics of Figure A-1 and Figure A-3.

The additional current mandated by the Figure A-2 amplifier was provided by modifying the power supply circuit shown in Figure A-3. Two 50 Ω resistors (0.5 W) are used instead of the 100 Ω (0.25 W) resistors of the original circuit.[2]
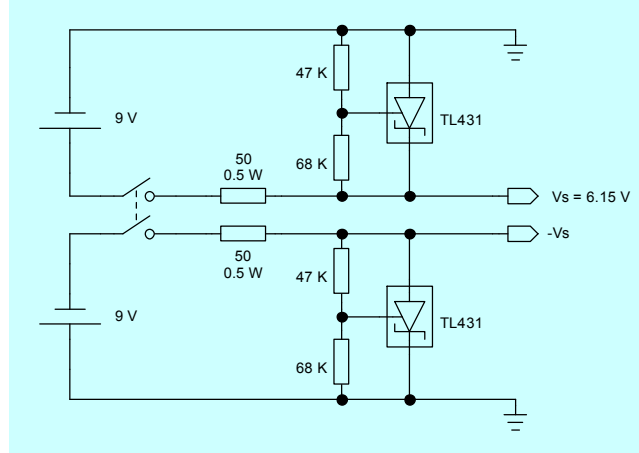

Figure A-3. Power supply circuit for charge pulse amplifier shown in Figure A-1.

In addition, the input to the pulse amplifier circuit was modified (see Figure A-4) so that a test pulse can be fed directly to the detector (FIND device) instead of to a separate test capacitor as in Figure A-1. The test pulse is attenuated such that the amount of charge across the FIND device electrodes is the same as that expected from a single neutron event; see Equation (1). In this way, the expected output pulse for the detector under test (rather than that of a test capacitor) can be observed directly, including any noise produced by the detector. The output of this attenuator circuit is fed to the "Detector In" input of the charge pulse amplifier circuit of Figure A-1.
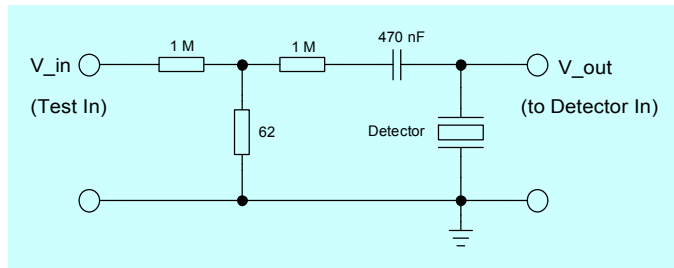

Figure A-4. Attenuator circuit for applying test pulse directly to the detector.

The resistors in the above attenuator circuit were selected for a detector using hBN film sample OUT111 (sample resistance $R_S \approx 25$ kΩ). The top two resistors in Figure A-4 are both $R_A = 1$ MΩ, and the lower resistor is $R_B = 62$ Ω. Ignoring the 470 nF capacitor, this resistor and detector combination form a so-called T-pad attenuator, with a DC attenuation of

$$\frac{V_{out}}{V_{in}} = \left[\left(1 + \frac{R_A}{R_S}\right) \cdot \left(1 + \frac{R_A}{R_B}\right) + \frac{R_A}{R_S} \right]^{-1}. \tag{A-1}$$

For R_S, $R_B \ll R_A$, the DC output impedance of such a T-pad attenuator will equal R_S (i.e., the charge pulse amplifier circuit will "see" a resistance of R_S) and the DC input impedance ("seen" by the "Test In" source) will be R_A. The 470 nF capacitor in Figure A-4 blocks the DC detector bias signal of Figure A-1 and keeps it from being applied to the "Test In" source. Note that values of the attenuator circuit components will depend on the sample resistance and the desired attenuation level.

APPENDIX B
CORONA TRIODE FEEDBACK CIRCUITS

Determination of the carrier mobility from Equation (10) based on measurements with the corona triode apparatus of Figure 8 require constant corona and sample currents (see the CARRIER MOBILITY MEASUREMENT METHODS section for further explanation). Few constant-current high-voltage power supplies are available commercially, particularly at the low current values (corona currents of a few microamps, and sample currents as low as nanoamps) typical for these measurements. The feedback circuits of block diagrams in Figure B-1 and Figure B-2 were therefore designed and built for this purpose. Detailed schematics of the various circuit sections are shown in Figure B-3 through Figure B-8.

The Applied Kilovolts high-voltage (HV) power supply of Figure B-1 includes a current monitor output V_{I-mon}, where 10 V corresponds to the maximum current of 400 μA. The polarity of the high-voltage output is reversible. The output voltage (0 to ±20 kV) is set by the control voltage V_{cont} (0 to 10 V). The Trek 609-3 HV amplifier of Figure B-2 amplifies its control voltage (0 to ±10 V) by a factor of 1000. For both feedback circuits, the supply voltage V_o must have a low noise level (i.e., a switching power supply is unsuitable).

The control section of Figure B-4 uses proportional/integral (PI) control to maintain V_{I-mon} equal to V_{PI-in} (shown as V_PI-in in this figure), and thus maintains a constant corona or sample current. V_{PI-out} serves as the HV power supply control voltage when the feedback circuits are operated in constant-current mode (see Figure B-7 and Figure B-8). The proportional gain is 5.6K/100K, or 0.056. The integration or integral time is 100K × 2.35 μF, or 235 ms. These values have been selected for use with the feedback circuit of Figure B-1; other values may be needed for use with the circuit shown in Figure B-2. Both of these cirucuits can also be operated in constant-voltage mode.

The display control section of Figure B-5 (applicable only to the feedback circuit shown in Figure B-1) uses Clare PBA150 and LCA125 solid-state relays to display low corona currents (up to 20 μA) on a 0.00 to 19.99 μA scale, and higher currents (up to 400 μA) on a 0.020 to 0.400 mA scale. Both the corona current (in μA or mA) and voltage (in kV) are displayed on Martel QM-140V digital panel meters.
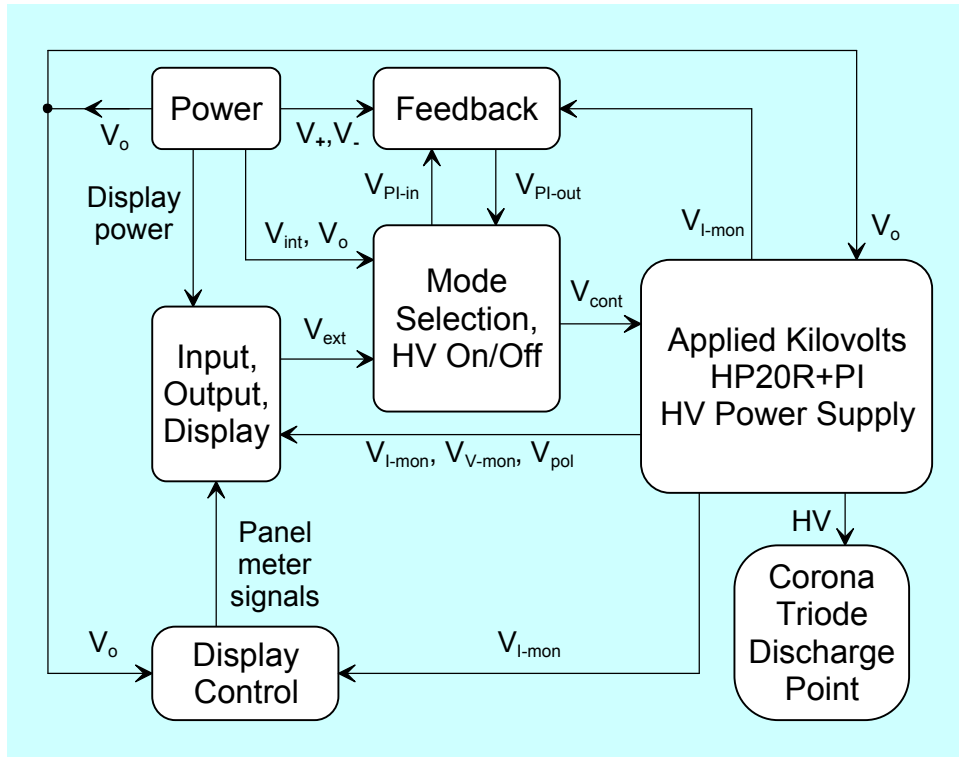
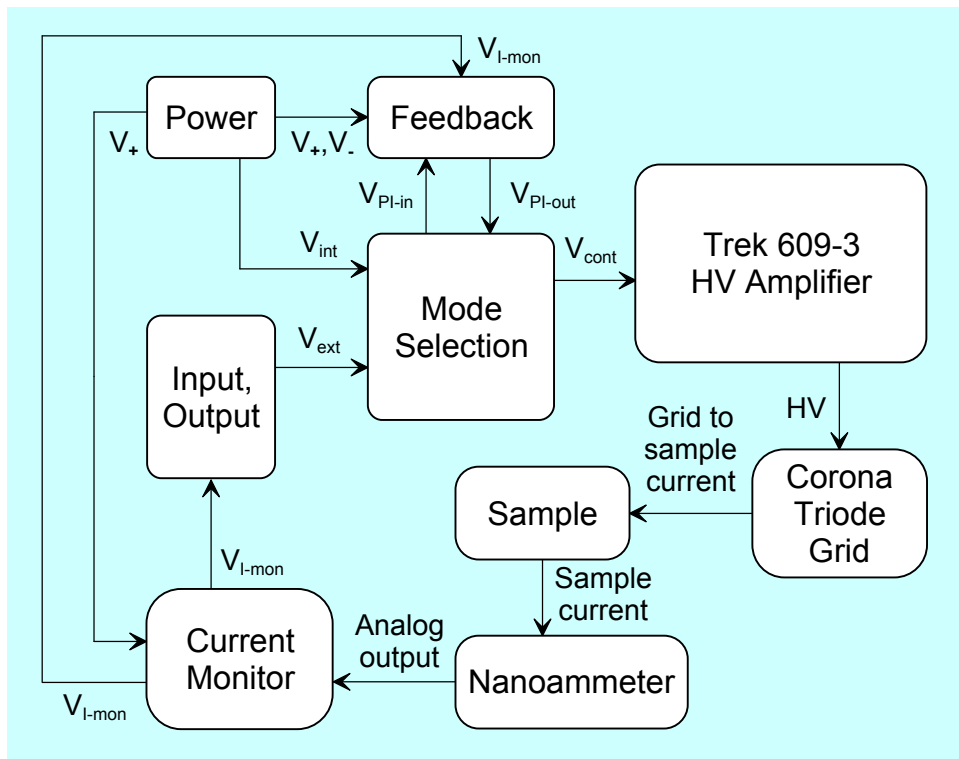Figure B-1. Constant-corona-current feedback circuit for corona triode.

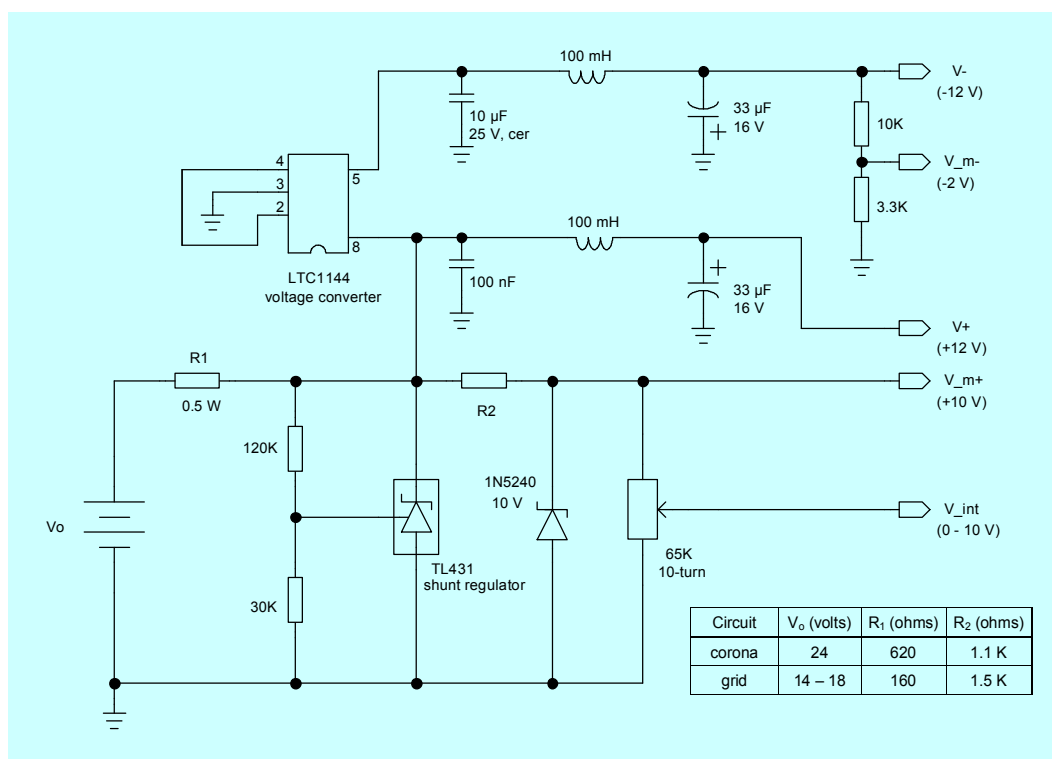Figure B-2. Constant-sample-current feedback circuit for corona triode.

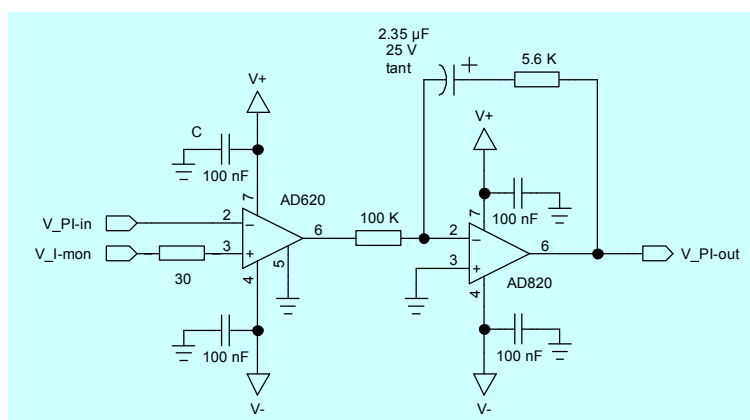Figure B-3. Power section of corona triode constant-current circuits.

Circuit	V_o (volts)	R_1 (ohms)	R_2 (ohms)
corona	24	620	1.1 K
grid	14 – 18	160	1.5 K

Figure B-4. PI control section of corona triode constant-current circuits.
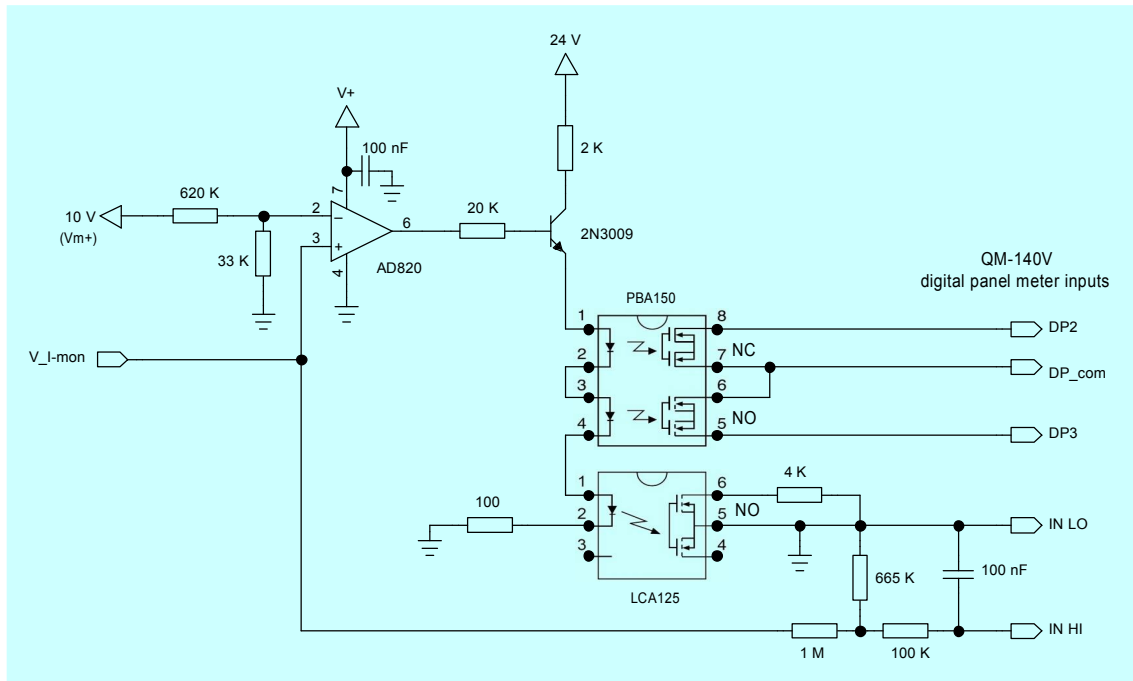
Figure B-5. Current display section of corona HV power supply control circuit.
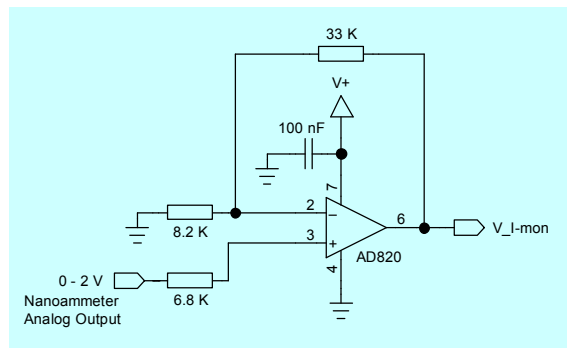

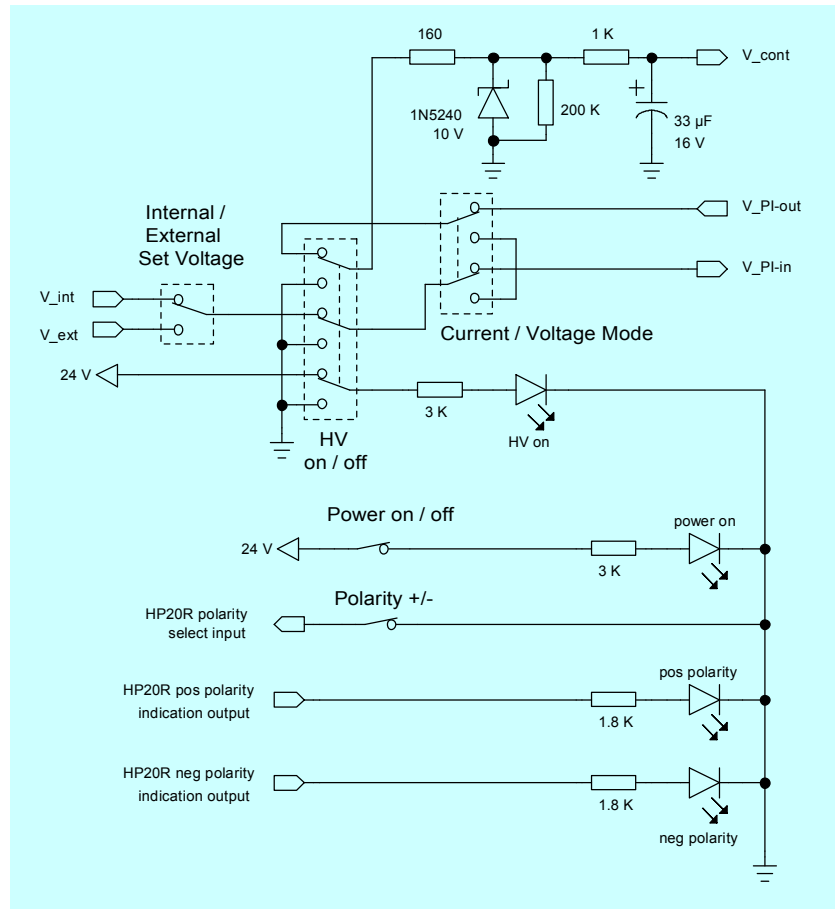Figure B-6. Grid current monitor section of grid HV power supply control circuit.

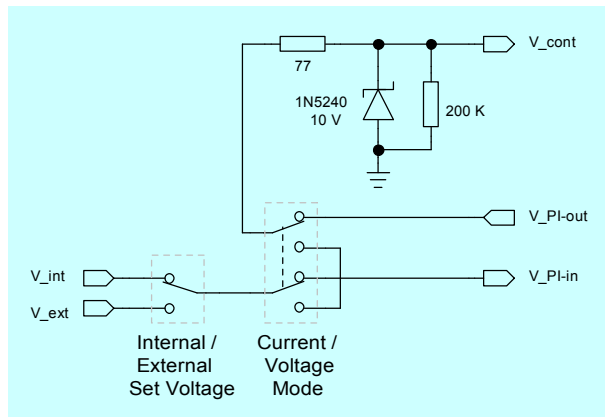Figure B-7. Mode select section of corona HV power supply control circuit.

Figure B-8. Mode select section of grid HV power supply control circuit.

APPENDIX C
ERRATA FOR SSC SAN DIEGO TECHNICAL REPORT 1921

Note the following corrections/clarifications to the previous FIND project report:[2]

Page 1, below Equation (1):

The alpha-particle energy should read 1.47 MeV, not 2.3 MeV.

Page 6, before Equation (5):

The sentence before the equation should read "Combining Equations 2 and 4, the carrier transit time is given by" instead of "Combining Equations 2 and 4, the carrier transit time I given by."

Page 8, Equations (7) and (8):

These equations are correct only for a thermal neutron absorption factor much less than one. Otherwise, the measured count rate will be the product of the neutron absorption factor, neutron flux, and detector area. The absorption factor is $(1-e^{-X})$, where X is the product of charge collection efficiency, macroscopic cross section, and sample thickness. Macroscopic cross section is the total thermal neutron cross section per unit volume.

Page 9, Equation (11):

The charge collection effieciency given in this equation is in the limit of a high level of carrier recombination or trapping (see the EXPECTED DETECTOR PERFORMANCE section of the present report for details).

Page 33, Table 7:

The actual etch rates are a factor of 10 smaller than stated in the table.

Page A-1, Figure A-1:

The resistors at ±Vs of TI-THS4031 are 4 Ω, not 200 Ω.

Page A-2, Figure A-2:

The polarity of the lower 9-V battery should be reversed (i.e., the positive side of that battery should be connected to ground).

REPORT DOCUMENTATION PAGE

Form Approved
OMB No. 0704-01-0188

1. REPORT DATE *(DD-MM-YYYY)*	2. REPORT TYPE	3. DATES COVERED *(From - To)*
September 2007	Final	

4. TITLE AND SUBTITLE

FILM IMPLEMENTATION OF A NEUTRON DETECTOR (FIND): CRITICAL MATERIALS PROPERTIES

5a. CONTRACT NUMBER

5b. GRANT NUMBER

5c. PROGRAM ELEMENT NUMBER

6. AUTHORS

W. C. McGinnis   R. Clarke
SSC San Diego   C. Cionca
                      University of Michigan

5d. PROJECT NUMBER

5e. TASK NUMBER

5f. WORK UNIT NUMBER

7. PERFORMING ORGANIZATION NAME(S) AND ADDRESS(ES)

SSC San Diego
San Diego, CA 92152–5001

8. PERFORMING ORGANIZATION REPORT NUMBER

TR 1957

9. SPONSORING/MONITORING AGENCY NAME(S) AND ADDRESS(ES)

Domestic Nuclear Detection Office
Department of Homeland Security
Washington, DC 20528-7100

10. SPONSOR/MONITOR'S ACRONYM(S)

11. SPONSOR/MONITOR'S REPORT NUMBER(S)

12. DISTRIBUTION/AVAILABILITY STATEMENT
Approved for public release; distribution is unlimited.

13. SUPPLEMENTARY NOTES

14. ABSTRACT

The FIND project is a research and development investigation of a new type of solid-state thermal neutron detector, potentially providing improvements in sensitivity, size, weight, power consumption, operator safety, transportability, and cost compared to current neutron detector technology. The objective of the project phase covered by this report was to develop a reproducible FIND device based on insulating boron nitride films or thin sheets, guided by the key materials properties needed for a workable device.

15. SUBJECT TERMS
Mission Area: Homeland Security
nuclear materials   neutron detection   thermal neutrons   boron nitride
carrier lifetime   carrier mobility   films

16. SECURITY CLASSIFICATION OF:			17. LIMITATION OF ABSTRACT	18. NUMBER OF PAGES	19a. NAME OF RESPONSIBLE PERSON
a. REPORT	b. ABSTRACT	c. THIS PAGE			W. C. McGinnis
U	U	U	U	75	19B. TELEPHONE NUMBER *(Include area code)* (619) 553–5610

Standard Form 298 (Rev. 8/98)
Prescribed by ANSI Std. Z39.18

INITIAL DISTRIBUTION

73513 Archive/Stock   (1)

Alan Janos, PhD   (1)
Program Manager
Transformational & Applied Research Directorate
Domestic Nuclear Detection Office
Department of Homeland Security
Washington, DC 20528-7100

SSC San Diego
San Diego, CA 92152-5001